

*Republic of Iraq
Ministry of Higher Education
and Scientific Research
University of Kerbala
College of Engineering*



A Study of Nano Zinc Oxide and Thermal Aging on Adhesion Force Between Rubber Composite and Steel Wire Cord

A Thesis

*Submitted to the College of Engineering / University of Kerbala in Partial
Fulfillment of the Requierments for the Degree of Master of Sience in
Mechanical Engineering – Applied Mechanics*

By

Saja Qasim Mohammed

B.Sc. 2013

Supervised By

Assist. Prof. Dr. Abdulkareem Abdulrazzaq ALhumdany

Assist. Prof. Dr. Muhannad Lafta AL-Waily

2017

١٤٣٨

بِسْمِ اللَّهِ الرَّحْمَنِ الرَّحِيمِ

نَرْفَعُ دَرَجَاتٍ مَّنْ نَّشَاءُ وَفَوْقَ كُلِّ ذِي عِلْمٍ

عَلِيمٍ

صَدَقَ اللَّهُ الْعَلِيُّ الْعَظِيمُ

سورة يوسف... آية (٧٦)

DEDICATION

To him ...

Who is our sun behind the cloud ...

Who holds my hands & makes me fly ...

Who listens to my words & even my feelings ...

Who learns me that working hard is the way for successful life...

To my lord, my leader who see us & sadly even for this moment we didn't see him...

For...

Imam Mahdi (AS)

To the fountain of patience, optimism and hope...

my dear father and my mother

To those who have demonstrated to me what is the most beautiful and helpful things...

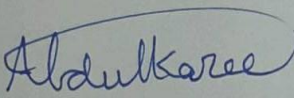
my brothers and sisters

I guide this research

Saja

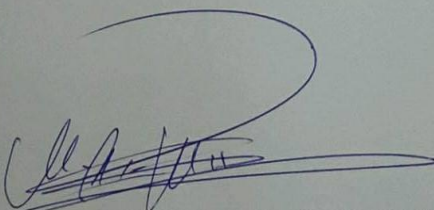
SUPERVISOR CERTIFICATE

We certify that this thesis entitled "A Study of Nano Zinc Oxide and Thermal Aging on Adhesion Force Between Rubber Composite and Steel Wire Cord" which is prepared by "Saja Qasim Mohammed" under our supervision at the University of Kerbala / College of Engineering-Mechanical Engineering Department in partial fulfillment of the requirements for the degree of Master of Sciences in Mechanical Engineering /Applied Mechanics.

Signature: 

Name: Assist. Prof. Dr. Abdulkareem Abdulrazzaq ALhumdany
(Supervisor)

Date: 2 / 11 / 2017

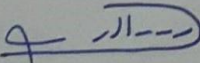
Signature: 

Name: Assist. Prof. Dr. Muhannad Lafta AL-Waily
(Supervisor)

Date: 27 / 11 / 2017

LINGUISTIC CERTIFICATE

I certify that the thesis entitled "A Study of Nano Zinc Oxide and Thermal Aging on Adhesion Force Between Rubber Composite and Steel Wire Cord" which has been submitted by "Saja Qasim Mohammed" has prepared under my linguistic supervision. Its language has been amended to meet the English style.

Signature: 

Name: Dr. Nabeel Mohammed Al-Zurfi

(Linguistic advisor)

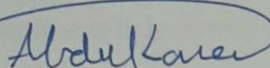
College of Engineering

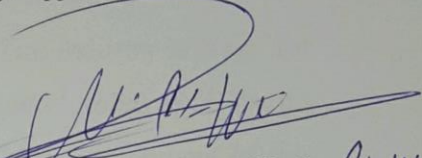
University of Kufa

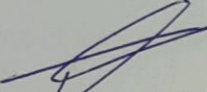
Date: 22/ 11 / 2017

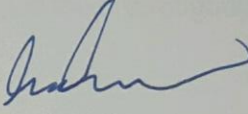
CERTIFICATE OF THE EXAMINING COMMITTEE

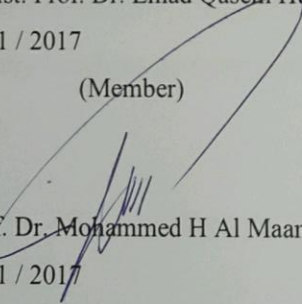
We certify that we have read the thesis entitled "A Study of Nano Zinc Oxide and Thermal Aging on Adhesion Force Between Rubber Composite and Steel Wire Cord" and as an examining committee, examined the student "Saja Qasim Mohammed" in its content and in what is connected with it, and that in our opinion it is adequate as a thesis for degree of the Master of Science in Mechanical Engineering / Applied.

Signature: 
Name: Assist. Prof. Dr. Abdulkareem ALhumdany
Date: 21 / 11 / 2017
(Supervisor)

Signature: 
Name: Assist. Prof. Dr. Muhannad Lafta
Date: 22 / 11 / 2017
(Supervisor)

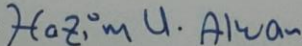
Signature: 
Name: Assist. Prof. Dr. Emad Qasem Hussein
Date: 21 / 11 / 2017
(Member)

Signature: 
Name: Dr. Sadiq Jaffar Aziz
Date: 23 / 11 / 2017
(Member)

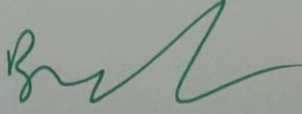
Signature: 
Name: Prof. Dr. Mohammed H Al Maamori
Date: 22 / 11 / 2017
(Chairman)



Approval of Mechanical Engineering
Department

Signature: 
Name: Dr. Hazim Umran Alwan
(Head of Mechanical Engineering Dept.)
Date: 26 / 11 / 2017

Approval of Deanery of the College of
Engineering / University of Kerbala

Signature: 
Name: Assist. Prof. Dr. Basim Khalil Nile
(Dean of the College of Engineering)
Date: 26 / 11 / 2017

ACKNOWLEDGMENT

Praise be to Allah for helping me in everything, how has bestowed upon me a valuable opportunity that I have dreamed of for so long.

I would like to thank my supervisors *Asst. Prof. Dr. Abdulkareem ALhumdany*.

My thanks to the staff in the State Company for Tire Industry in Najaf for their patience and help during this work especially *Fadhel Abbas Hadi* for his continuous efforts, guidance, and advice throughout the development of this project.

I would like to express my sincere appreciation to *Asst. Prof. Dr. Luay Al-Ansari* for his help, immense knowledge, and guidance throughout the preparation of the work described in this thesis.

Most importantly, I would like to express my thanks and gratitude to my parents, my brothers and my sisters for their unconditional support, love, and affection.

ABSTRACT

Adhesion of rubber compound to steel cord is of extreme importance to the rubber industry. The present study aims to study of nano-zinc oxide and thermal effect on the adhesion force of rubber-tire cord interface. This study includes experimental and numerical parts.

Due to a temperature increase through running tires, the energy of adhesion will differ as compared with the initial state. To study rubber-cord interface at raised temperatures, the T-pull test method is used. In this research, T-adhesion of samples is evaluated at different temperature values 25, 50, 75, and 100 °C. Also, tensile properties and hardness are studied to help the designer to make better and stronger tires.

Eleven different rubber compounds were prepared by a two-roll mill and laboratory presses to study the effects of common ingredients on the rubber-tire cord interface. One compound has conventional zinc oxide as an activator with 8pphr (part per hundred rubber) concentration. Eight compounds have nano-zinc oxide with 0.2, 0.6, 1, 1.4, 1.8, 2.2, 2.75, 4 pphr. The other two compounds have nano-zinc oxide with 2.2pphr, one has cobalt stearate with 2pphr instead of 1pphr and the other has carbon black with 65pphr instead of 50 pphr.

The numerical part is implemented using the finite element method (FEM) operating on ANSYS APDL. Vr 16.1 to estimate the pull-out-force which is needed to pull out the cord of steel from the mass of rubber for all types of compounds. The numerical simulation results are compared with those of experiment.

The results obtained from the experimental work show that the increased temperature leads to decrease the adhesion in the rubber-tire cord interface. The

replacement of conventional zinc oxide by nano-zinc oxide leads to improve the adhesion force by 21%, reduce the amount of zinc oxide by 72.5% and the tensile strength by 45.11%. It also leads to reducing the cost of the compounds because the price of nano-zinc oxide is approximately equal to the price of conventional zinc oxide.

The numerical results show that the pull-out force is increased by 22.8%. When compared with the experimental result, the error percentage is found to be 9.7%.

LIST OF CONTENTS

Abstract	I
List of Contents	III
List of Abbreviation	VII
List of Figures	VIII
List of Tables	XI
 <i>Chapter one – Introduction</i>	
1.1 General	1
1.2 Radial Tire Components.....	2
1.3 Vulcanization Processes.....	3
1.4 Adhesion.....	4
1.4.1 Adhesion Theories.....	4
1.4.1.1 Diffusion Theory.....	4
1.4.1.2 Adsorption theory.....	5
1.4.1.3 Electrostatic Theory.....	5
1.4.2 Adhesion Between Rubber and Steel Cord.....	6
1.5 Hardness.....	9
1.6 Tensile Properties.....	10
1.7 Thesis Objectives.....	11
1.8 Layout of Thesis.....	12

Chapter two – Literature Review

1.1 General.....	13
2.2 Concluding Remarks.....	18

Chapter three – Experimental Work

3.1 General.....	20
3.2 The Used Materials.....	21
3.2.1 Standard Malaysian Rubber (SMR20).....	22
3.2.2 Zinc Oxide.....	22
3.2.3 Nano-Zinc Oxide.....	23
3.2.4 Carbon Black.....	23
3.2.5 Steel Cord.....	23
3.3 Compounding Recipes.....	25
3.4 Preparing and Mixing Compound Materials.....	28
3.5 The Fabrication Specimen and Testing Work.....	30
3.5.1 Vulcanization Rubber Specimen.....	30
3.5.2 Hardness Test.....	31
3.5.3 Tensile Test.....	32
3.5.4 Adhesion Test.....	35

Chapter four – Numerical work

4.1 General.....	38
------------------	----

4.2 Finite Element Method.....	38
4.3 Finite Element Software Package ANSYS 16.1.....	38
4.3.1 Defining Element Type.....	39
4.3.2 Defining material properties.....	40
4.3.3 Draw model geometry.....	41
4.3.4 Mesh generation.....	42
4.3.5 Create of contact.....	43
4.3.6 Applying a load and boundary condition.....	45

Chapter FIVE – results and discussion

5.1 General.....	47
5.2 Experimental Part.....	47
5.2.1 Adhesion.....	48
5.2.2 Hardness.....	53
5.2.3 Tensile Properties.....	55
5.2.3.1 Tensile Strength.....	55
5.2.3.2 Modulus at 300%.....	58
5.2.3.3 Elongation at Break.....	59
5.3 Numerical part.....	65

Chapter six – Conclusions and Recommendations

6.1 Conclusions.....	72
----------------------	----

6.2 Recommendations.....73

References.....74

Appendices

The Results of Tensile Test.....A-1

LIST OF ABBREVIATION

Sample	Definition	Unit
6PPD	Anti-Ozinants	
ASTM	American Society of Testing and Materials	
BR	butadiene rubber	
Co ²⁺	Cobalt ion	
CRI	Cure rate index	(minute) ⁻¹
CTP-100	N - (cyclohexylthio) phthalimide (phthalimide)	
CuO	Copper oxide	
CuS	Copper sulfide	
DCBS	Accelerator	
FEM	Finite element method	
IRHD	International rubber hardness degree	
Nano-ZnO	Nano-Zinc Oxide	
NBR	Nitrile Rubber	
NR	Natural Rubber	
pphr	Parts per hundred rubber	
RF	Resorcinol formaldehyde resin	
SBR	Styrene Butadiene Rubber	
SMR20	Standard Malaysian rubber	
tc90	Optimum cure time	minute
Ts2	Scorch time	minute
Zn ²⁺	Zinc ion	
ZnO	Zinc oxide	
ZnS	Zinc sulfide	

LIST OF FIGURES

Figure No.	Title	Page No.
1.1	Components of Radial Tire	2
1.2	Network Formation	3
1.3	Steps for Mechanism of Rubber-Brass Bonding	8
3.1	Steel Cord Components/ (1) Filament, (2) Strands, (3) Cord, (4) Spiral Warp	24
3.2	The Cross Section of Steel Cord	25
3.3	Rolls Mill	28
3.4	Thermal Hydraulic Press	30
3.5	Hardness Disc	31
3.6	Dead load hardness tester	32
3.7	Tensile Sheet	33
3.8	Specimen Cutting Press	33
3.9	Dumbbell Specimen of Tensile Test	34
3.10	Monsanto T10 Tensometer	35
3.11	Mold of Adhesion Sample	36
3.12	Adhesion Specimen after Cleaning	36
3.13	Grips of Adhesion Specimen	37
4.1	SOLID185 Homogeneous Structural Solid Geometry	40
4.2	The Parts in (3D) Model for Rubber Block and Steel Wire	41
4.3	Mesh Generation for Rubber Block	42
4.4	Relationship Between Number of Element and Von-Misses Stress on Rubber Block	43
4.5	CONTA174 Geometry	44
4.6	TARGE170 Geometry	45
4.7	Define load and Boundary Condition	46

5.1	Pull-Out Force of (A) Compound at Different Temperatures	48
5.2	Pull-Out Force of (B) Compounds at Different Temperatures	50
5.3	Pull-Out Force of B6 Compound and (A) Compound at Different Temperatures	51
5.4	Pull-Out Force of (B6) Compound and (C) Compound at Different Temperatures	52
5.5	Hardness Rate of (B) Compounds	54
5.6	Hardness Rate of (A), (B6) and (C) Compounds	54
5.7	Tensile Strength for (B) Compounds	57
5.8	Tensile Strength for (A), (B6) and (C) Compounds	57
5.9	Modulus at 300% for (B) Compounds	58
5.10	Modulus at 300% for (A), (B6) and (C) Compounds	59
5.11	Elongation at Break for (B) Compounds	60
5.12	Elongation at Break for (A), (B6) and (C) Compounds	60
5.13	Comparing the Tensile Strength Between (B6) and (D) Compounds	62
5.14	Comparing the Modulus at 300% Between (B6) and (D) Compounds	63
5.15	Comparing the Elongation at Break Between (B6) and (D) Compounds	63
5.16	Comparing the Hardness Between (B6) and (D) Compounds	64
5.17	Comparing the Pull-Out Force Between (B6) Compound and (D) Compound	65
5.18	Moving Cord in Rubber Block	66

5.19	Comparison between Numerical and Experimental Pull-Out Force of (B) Compounds	68
5.20	Comparison between Numerical and Experimental Pull-Out Force of A, B6, C and D Compounds	69
5.21	Steel Wire in (A) Rubber Block After Extrusion	70
5.22	Steel Cord in (D) Rubber Block After Extrusion	71

LIST OF TABLES

Table No.	Title	Page No.
3.1	Type of Materials Used in the Experiments	21
3.2	Rubber Compound Recipe of (A) in pphr	26
3.3	Rubber Compound Recipe of (B) in pphr	26
3.4	Rubber Compound Recipe of (C) in pphr	27
3.5	Rubber Compound Recipe of (D) in pphr	27
3.6	Mixing Schedule	29
5.1	Pull-Out Force Values at Different Temperature of (A) Compound.	48
5.2	Pull-Out Force Values at Different Temperature of (B) Compounds	50
5.3	Pull-Out Force Values at Different Temperature of (C) Compound	52
5.4	Results of Hardness Test of (B) Compounds	53
5.5	Results of Tensile Test (A), (B) and (C) Compounds	56
5.6	The Laboratory Control Limit for 1k4100 (A) Compound	61
5.7	Results of Tensile Test for (D) Compound	62
5.8	Pull-Out Force Values at Different Temperature for (D) Compound	64
5.9	Pull-Out Force of Experimental and Numerical work with Percentage Error Between Them	68



CHAPTER ONE
INTRODUCTION

Chapter 1**INTRODUCTION****1.1 General**

Elastomers (natural and synthetic rubber) are a shapeless polymer to which numerous components are added to refer to as a compound. These materials become rubber compound after heating and vulcanization. The macromolecular network construction of elastomeric materials gives the ability of these materials to endure large strain [1]. Nonlinear elastic deformations of up to 500-800%. Unless destruction occurs, after removal of the load they will return to their original shape.

Elastomers are used in many applications of engineering due to their low cost wide availability, dissipating energy, resiliency, long service life, light weight and they can be simply molded into any shape. Applications of rubber are presently used in coatings, cables, medical/dental, tires, optical devices, engine mounts, and gaskets .

The tire is undoubtedly one of the most important examples of rubber applications. Tire needs the rubber to undergo fast cyclic deformations at a certain frequency to improve its quality. Reinforcement fibers and cords are used to improve stiffness, strength, stability, uniformity in tires and production radial-ply tires consisting of a composite structure of metallic wires and rubber [2]. The quality depends highly on the strength of adhesion between the rubber and the wire.

1.2 Radial Tire Components

The tire is a composite of complex elastomer, fibers, textiles and steel cord. Figure (1.1) shows a part of a radial tire which has a body ply cords at 90° on the centerline of the tread. Each part performs its function. The steel belts part lying under the tread used to provide strength and stability to the tread, reduce rolling resistance as well as contain the air pressure [3, 4].

This part consists of reinforcing materials (steel, polyester, rayon and nylon) and rubber compound which has natural rubber, fillers, plasticizers, chemical for vulcanization, anti-aging agents and other chemicals.

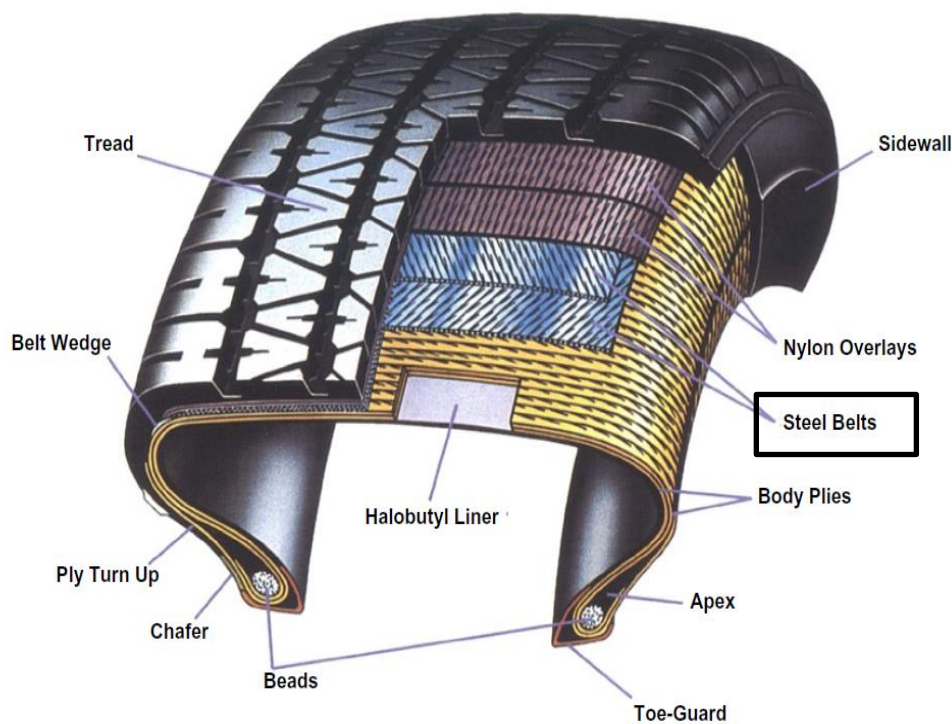


Figure 1.1: Components of Radial Tire [5].

1.3 Vulcanization Processes

The rubber in its original state is generally not very strong. It does not maintain its shape after a large deformation, having its consistency as a gum. It cannot be made without vulcanization or curing. Vulcanization is a process usually applied to rubbery or elastomeric materials. It can be defined as a process which increases the retractile force and reduces the amount of permanent deformation residual after removing the deforming force. Thus, vulcanization decreases plasticity while it increases elasticity [3].

Vulcanization chemically produces network connection by inserting crosslinks between the polymer chains, Figure (1.2). The process is generally carried out by heating elastomeric materials with vulcanizing agents under pressure. The sulfur is widely used as the vulcanizing agent.

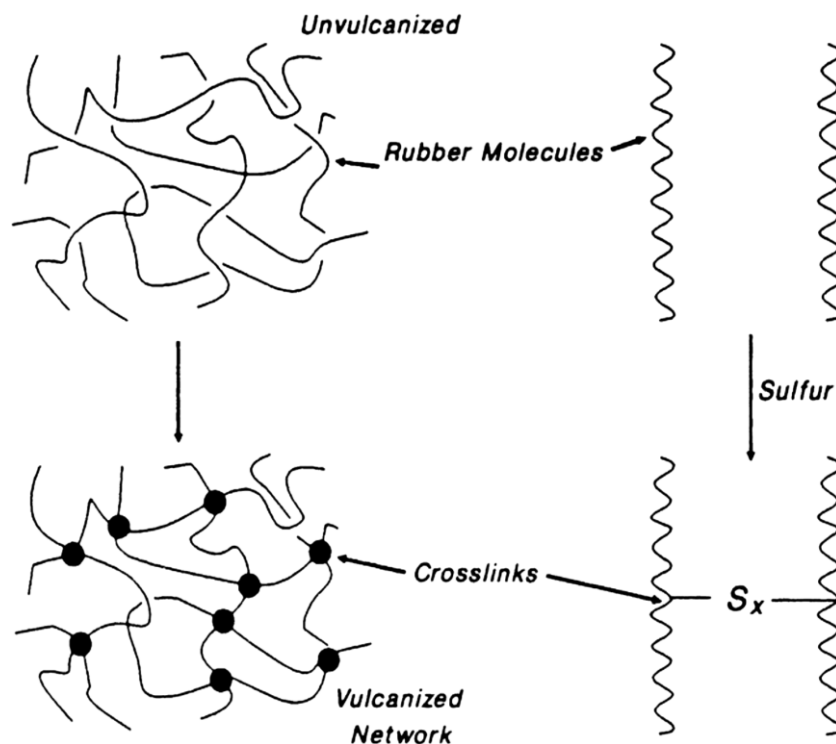


Figure 1.2: Network Formation [3].

The sulfur must be well dispersed in the rubber to get on the effective vulcanization. Incomplete dispersion causes inhomogeneities in the final vulcanizate. Dispersion is simplified if there is a high solubility of sulfur in the elastomer [6].

1.4 Adhesion

Brass-coated steel cords are widely used in tire manufacturing. The addition of these cords leads to a better tire performance. In order to gain the best tire performance, these tire cords must adhere well with the surrounding rubber compound. For improved performance in radial tire technology, it is necessary to make advancement in the rubber-tire cord adhesion and other mechanical properties of the final compound of additives and various adhesion promoters [5]. However, the theory and the mechanism of this adhesion of the sulfide layer at the rubber-tire cord interface have not been fully understood yet.

1.4.1 Adhesion Theories

1.4.1.1 Diffusion Theory

The most widely used and successful theory which explains tack or autohesion is the diffusion theory of adhesion of Voyutskii [7]. He suggested that if two rubber surfaces were in sufficiently close contact, part of the long chain molecules on the surface would diffuse across the interface. The surface molecules will interpenetrate and eventually the interface will disappear and the two parts will have become one. For such an interdiffusion to take place, the molecules must be relatively mobile, which further requires that the rubbers must be above their glass transition temperature and that there should not be any appreciable degree of crosslinking in either of them. There is some experimental evidence that such diffusion takes place across the interface

during a relatively short time of contact. However, the diffusion theory does not explain the variation of autohesion with the temperature of measurement, or the increase in autohesion with increase in contact pressure [7].

1.4.1.2 Adsorption theory

Rubber surfaces experience varying degrees of adhesion when brought into contact. The physical forces of adhesion are generally thought to arise from two main sources: one electrostatic and the other van der Waals type short range attraction. The adsorption theory attributes bond strength to the formation of intermolecular forces of attraction or van der Waals forces between the surface molecules. According to this theory tack or autohesion is purely a surface phenomenon and there is a direct correlation between the energy of adsorption and the autohesive bond strength and as polarity increases there should be a proportional increase in the bond strength. However, in practice, such a correlation does not exist and highly polar rubbers tend to have less autohesion [8].

1.4.1.3 Electrostatic Theory

No two surfaces are absolutely identical and there will be some contact electrification. The electrostatic theory considers the two surfaces to be bonded as the two plates of an electrostatic condenser, and is due to Deryaguin. According to this theory adhesion occurs due to the electrostatic forces formed by interaction between the substrates. This theory explains the pressure dependence of tack/autohesion very well but it does not explain why raw and compounded rubbers lose most tack/autohesion as they are cured and brought into molecular contact under pressure. Further this theory is also not successful in explaining the time and temperature dependence of the tack/autohesion. By

using potential contrast scanning electron microscopy, the existence of an electric double layer at the polymer interface has been demonstrated [9].

1.4.2 Adhesion Between Rubber and Steel Cord

Bonding rubber to metal is a complex compound of metallurgy science, rubber chemistry, adhesion science and engineering process with many of the interactions. Natural rubber compounds don't directly adhere to steel metal, therefore, the usage of a thin brass coating of twisted steel cords is very important and to prevent rusting. Many researchers studied and proved the adhesion mechanism of natural rubber to brass. It has been established that a tough bond is formed between the brass surface and the rubber through the vulcanization process of the rubber.

Steel cord coated with a thin layer of brass is drawn during the forming process. The zinc ions (Zn^{2+}) diffuse to the surface and are oxidized to a zinc oxide (ZnO) layer and very small amounts of copper oxide (CuO) film is created. Through vulcanization, active sulphur in rubber compound touches the copper in the brass coat and a strong copper sulfide (CuS) bonds with some zinc sulfide (ZnS) are shaped during sulphidation between the cords and the rubber compound [2]. Copper sulfide domains are formed on the surface of the brass film during the vulcanization reaction. These domains have a high specific surface area and they are produced within the wire coat compound before the polymer is cross-linked into an elastomeric network [3,10].

During vulcanization, (ZnS) does not bond because it does not grow rapidly enough, therefore it cannot interlock with the polymer. However, degradation of the wire-rubber adhesive bond is catalyzed by Zn^{2+} ions, which diffuse through the interfacial CuS film. This will finally result in an excess of either ZnS or ZnO. The Zn^{2+} ions will travel to the surface, with the following

drop in the mechanical interlocking of the CuS domains and rubber subsequent by degradation of adhesion. To reduce the migration Zn^{2+} ions through the CuS interface addition of cobalt, cobalt ions (Co^{2+}) reducing the conductivity of the ZnO [3,10]. The mechanism of this process is illustrated in Figure (1.3).

For reducing Zn^{2+} ions such as replacing conventional ZnO by nano-ZnO, since nano-ZnO has a very small particle size (10-100 nm) and its surface area is higher than that of conventional ZnO [11]. Low level from nano-ZnO improves physical properties as compared with the level of conventional ZnO.

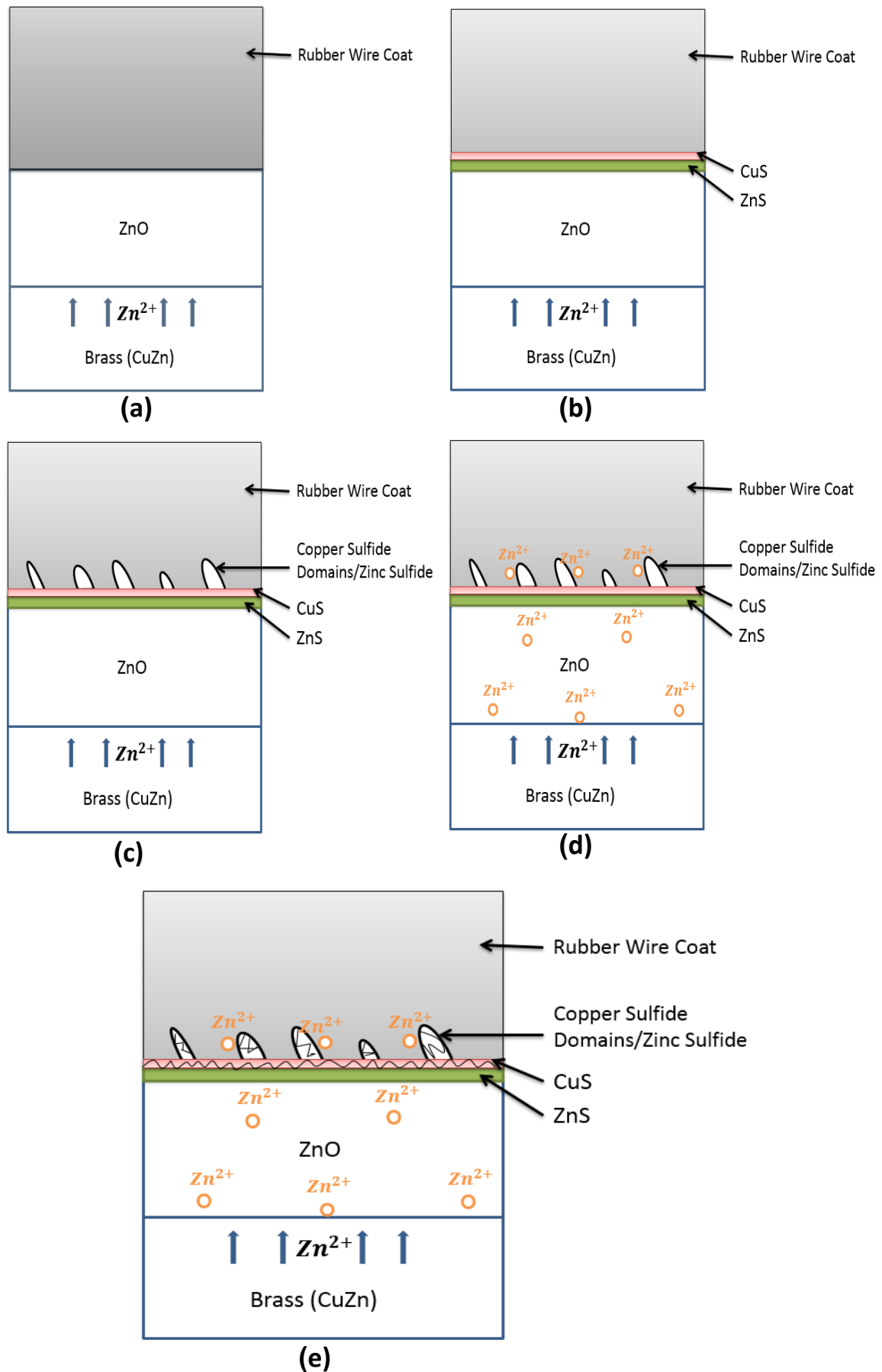


Figure 1.3: Steps for Mechanism of Rubber-Brass Bonding.

1.5 Hardness

Hardness is one of the most significant properties which determine the suitability of any rubber part for its designated end purpose. It is defined as the relative resistance of the surface of the material to depression.

For measuring international hardness of rubber in the Company for Tire Industry is according to ASTM D1415 [12]. International Hardness depends on the difference in penetration depth of a specified dimension ball with the rubber. This consists of a small initial force and a much larger final force. The differential penetration is taken at a specific time and converted to a hardness scale value, called; international rubber hardness degree (IRHD). This test is used for measuring the hardness of vulcanized rubber.

Approximately international hardness is related to the modulus of elasticity. However, for highly non-linear rubbers this relationship is not effective [12].

The relationship between the Young's modulus and the penetration is approximately expressed by equation 3.3 [12].

$$\frac{F_i}{E} = 1.9 r_a^2 \left(P_e \frac{P_e}{r_a} \right)^{1.35} \quad \dots\dots\dots 1.1$$

Where

F_i : Indenting force (N)

E : Young's modulus (Pa)

r_a : Radius of a ball (mm)

P_e : Differential penetration (mm)

The values of hardness are in the range between 0 and 100 IRHD [12].

1.6 Tensile Properties

Rubber is basically an incompressible substance that deflects by changing shape rather than changing volume. When strains are very low, the ratio between resulting stress to the applied strain is a constant (Young's modulus). Therefore, Hooke's law is valid within this proportionality limit. However, as the strain increases, this linearity finishes and Hooke's law is non-applicable. The compression and tension stresses are then different so that the relation between them of rubber does not obey Hooke's law [13].

Stress-strain properties include stress and strain at the break point and the modulus at the determining strain such as at strain equals to 300% [14]. These properties are significant for determining the elasticity and the breaking resistance of the material.

Stress-strain properties of rubber compounds are usually measured under tension test according to ASTM D412 [14]. The test sample is stretched until it breaks, and record the values of tensile strength, elongation and modulus at determined strain [14].

a. Tensile Strength

Tensile strength in rubber compound is specified as the maximum tensile stress applied in stretching a test sample of rubber compound to rupture. The tensile strength can be taken in consideration either together or separately with the elongation and modulus for any specific compound in defining an optimum state of cure [14].

The relation between tensile strength and the force which is affected on the test sample of rubber is [14]:

$$TS = \frac{F_{BE}}{A} \quad \dots\dots\dots(1.2)$$

Where

TS: tensile strength, the stress at rupture (MPa)

F_{BE} : the force magnitude at rupture (MN)

A: cross-sectional area of the unstrained test sample (m^2).

b. Elongation at Break

Elongation describes the ability of the rubber compound to stretch without breaking. It is equal to the difference between the final and initial lengths expressed as a percentage of the last, it can represent as [14]:

$$E_L = \frac{L-L_0}{L_0} \times 100 \quad \dots\dots\dots(1.3)$$

Where

E_L : The elongation in percent (of original bench mark distance).

L : Observed distance between bench marks on the extended test sample.

L_0 : Original distance between bench marks.

c. Modulus

Modulus is the amount of stress required for a given elongation and is used as a supplement to modulus in comparative evaluations. This value is determined by the tensile test [14].

1.7 Thesis Objectives

The main objective of this thesis is to study of nano-zinc oxide and thermal effect on the adhesion force between rubber compound and steel tire cord.

1.8 Layout of Thesis

This thesis is divided into six chapters, chapter one is an introductory chapter which contains a general introduction to the history of elastomeric materials and a mechanism for adhesion between rubber and steel cord, as well as the thesis objectives.

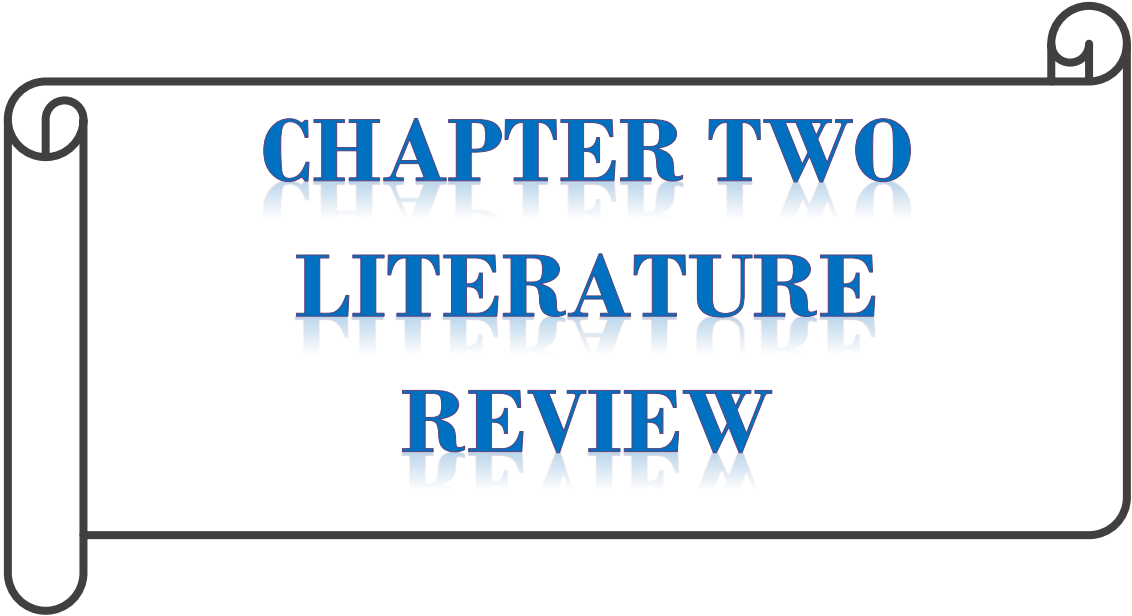
Chapter two contains the literature review for the adhesion force between rubber and steel tire cord as well as a review to reduce ZnO levels in the rubber compound. The effect of nano-ZnO on rubber compound is also reviewed.

Chapter three presents the detailed experimental work. The materials used in this thesis are reviewed. The fabrication of test specimens and the manufacturing method are demonstrated. The basic experiments performed are adhesion tests under different temperatures, the tensile test and hardness test. These tests were done for the rubber compound used in this thesis.

Chapter four presents the detailed numerical work by using finite element software Package ANSYS 16.1 for pull-out force in steel wire embedded in rubber block.

In chapter five, the results are reviewed and discussed for both the experimental and numerical data of the proposed models. The discussions include the effect of nano-ZnO, cobalt stearate and carbon black percentage upon the rubber compound materials specimens.

Finally, in chapter six, the main findings and contributions of the present thesis are summarized and some recommendations and suggestions for future work are given.



CHAPTER TWO
LITERATURE
REVIEW

LITERATURE REVIEW

2.1 General

This chapter reviews some of the researches that are mostly related to the scope of the present work. In the following paragraphs, the researches that have been conducted on rubber sorted according to the history of each one.

Gyung et al., 1999 [15] studied the effect of ZnO concentration at the surface of brass coated steel wire on the adhesion force between rubber and steel cord. They found that pull-out force in a sample of cord which has higher ZnO concentration is poorer than that of lower ZnO concentration. From the thermal aging point of view, the pull-out force decreased with increasing aging time and that for the first cord is lower than second cord.

Seo and Jeon, 2001 [16] investigated the effect of cure time (tc90) on the adhesion force between rubber and brass-plated steel cord. To study different cure time (25%, 50%, 100%, 200%, 400%) of tc90. They found that the pull-out force after vulcanization increased up to one-half of tc90 followed by a slight increasing in tc90. Afterward, further increase in cure time leads to a decrease in the pull-out force. The prolonged vulcanization causes a severe growth of CuS and a large amount of dezincification at the adhesion interface. A shorter tc90 makes CuS does not occur in the adhesion interface. All these reasons may be made the degradation of rubber compound attached to the adhesion interface. During studying thermal aging of the samples, they found

that pull-out force decreased with increasing heat in comparison with that of the unaged.

Al Maamori and Hasan, 2002 [17] studied the effect of different content sulfur (0.5,1,1.5,2,2.5,3) pphr, carbon black (25,45,65,85,100) pphr and cobalt stearate (0,0.5,1,1.5,2) pphr on mechanical properties of NR. They found that the best adhesion force is in 2.5 pphr sulfur, 85 pphr carbon black and 1 pphr cobalt stearate. When using resorcinol formaldehyde resin (RF) there is increasing in adhesion force from 450 N to 616 N between rubber and steel wire.

Seo and Jeon, 2003 [18] presented the effect of cure level (under cure, optimum cure, over cure) of composites on adhesion between rubber and steel tire cord. Short cure time at low temperature brings about under-cure (130°C, 20min and 150°C, 5min), over-cure composites cured at high temperature or for a long time (150°C, 80min and 170°C, 20min) and cure the condition for an optimum cure at (150°C, 20min). They found that the highest pull-out force for adhesion T sample is at optimum cure because the cure time and cure temperature are enough to achieve a sufficient growth of the adhesion interface, a higher tensile property of rubber compound and proper crosslinking density of rubber.

Hiedman et al., 2004 [11] investigated the effect of conventional ZnO and nano-ZnO with a particle size (20-40 nm) on rubbers. They found that only one-tenth of the amount of nano-ZnO in comparing with conventional ZnO is necessary to achieve the same cure characteristics. Also, they found that replacement of conventional ZnO by nano-ZnO leads to an improvement of the properties of the rubber compound, especially the abrasion resistance and tear strength.

Jamshidi et al., 2005 [19] studied the effect of elevated temperatures, which are 25, 50, 75, 100, 125, 170 °C, on cord-rubber interface adhesion at vulcanized temperatures of 130, 140, 150, 160 °C. They found that in all cases, the increase in temperature causes a decrease in adhesion force and the best vulcanized temperature is at 150 °C.

Jeon, 2005 [20] investigated the effect of amounts of cobalt plating (0, 2 and 4%) in coated steel cord on adhesion on rubber compound. The adhesion T samples are aged thermally at 95 °C for couples of days (5, 10 and 15). The results showed that the optimum adhesion is for the unaged state of 2% cobalt plating and high pull-out force for all aged days also at 2% cobalt plating compared with brass-coated steel cord (without cobalt). An increase of cobalt plating up to 2% showed poor adhesion properties to the rubber compound compared to brass-plated steel cord.

Jeon et al., 2005 [21] presented the effects of cobalt salt and sulfur in rubber compounds on adhesion characteristics to the ternary-alloy-coated steel cord with 2% cobalt plating amount. They used three rubber compounds, the first one had a 4 pphr sulfur loading without cobalt salt, the second one had 4 pphr sulfur with 0.4 pphr cobalt salt loading and the third one had 8 pphr sulfur with 0.4 pphr cobalt salt. They found that increasing cobalt salt leads to increase the cure rate, cross-link density, hardness and modulus. Increasing sulfur loading at a constant loading of a cobalt salt increased the hardness and modulus. The pull-out force of adhesion T-sample increased significantly with increasing loading of cobalt salt in the rubber compound with constant sulfur loading, while it decreased with increasing sulfur concentration into the rubber compound with constant cobalt salt loading. The pull-out force is decreasing after thermal aging and the optimum value of the second rubber compound.

Wang and Chen, 2005 [22] carried out an experimental work to study the effect of conventional ZnO with 1, 2, 3, 4, 5 pphr concentration and nano-ZnO with same concentration on mechanical properties and cure characteristics in styrene butadiene rubber (SBR) systems. They found that the highest mechanical properties are at 5pphr conventional ZnO filled systems and 1pphr of nano-ZnO. It can be seen that nano-ZnO is the best among five systems, also cure characteristics (scorch time, cure time, minimum torque, maximum torque) prolong when using nano-ZnO and these properties improved the crosslinking density.

Harakuni, 2007 [5] studied the aging in heat and humidity effects on the rubber-steel cord interface of five experimental compounds. In these compounds, there is changing in cobalt and sulfur percentage. He found that in all compound form CuS at the interface is initially amorphous and both types of aging tend to crystallize. The continued aging causes a high crystalline CuS layer and this leads to degradation and separation from the metal surface as well as the formation of ZnO at the interface. The ZnO formed in excess tends to adhesion between rubber and steel tire cord detrimentally.

Sahoo et al., 2007 [23] studied the effect of conventional ZnO and nano-ZnO with an average particle size of 50 nm as cure activators for natural rubber (NR) and nitrile rubber (NBR). In this paper, the effects of 5pphr of conventional ZnO with 5 and 3 pphr of nano-zinc oxide are compared. They found that replacing conventional ZnO by nano-zinc oxide improves dynamic mechanical properties, mechanical properties and increased crosslink density. The tensile strength is improved by 80% for NR and 70% for NBR. At this replacement, the modulus at 300% is improved by 20% for NR and 30% for NBR at 5 pphr loading of nano-ZnO. At 5pphr of nano-ZnO, the maximum torque is increased with 12% for NR and 18% for NBR.

Jeon, 2008 [24] investigated the effect of sulfur loading in rubber compounds and various adhesion promoters (cobalt salt and zinc borate) on the adhesion between rubber compounds and brass-plated steel cords. He found that the pull-out force of adhesion samples decreased slightly with increasing the loading amount of sulfur in the rubber compounds containing cobalt salt or zinc borate. After thermal aging treatments, the adhesion improved by increasing loading amount of sulfur in the rubber compounds. In the rubber compounds containing cobalt salt, a cure rate is decreased with increasing loading amount of sulfur into rubber compounds, but the cure rate of a rubber compound containing zinc borate increased slightly with increasing loading amount of sulfur. The largest tensile strength is found in the rubber compounds containing zinc borate with a loading of 4 to 8 pphr of sulfur.

Ganjali et al., 2009 [25] presented the effect of nano-ZnO with a particle size of 30-70 nm and with a specific surface area of 39.7 m²/g on physical properties of NR/SBR blend with a ratio of 75/25. They found that mechanical properties (tensile strength, modulus of elasticity and abrasion resistance) can be largely improved by using 2 pphr of nano-ZnO. This result due to the increased interfacial interaction between the nanoparticles and rubber matrix, which occurs because of the reduction in size and increase in surface area.

Saad et al., 2009 [26] investigated the effect of carbon black used as filler with a loading of 40, 60, 80, 100 pphr on cure characteristics and mechanical properties. The results of this study showed that increasing of carbon black loading leads to increase the difference between the minimum and maximum torque. The cure time and the scorch time decreased while the cure rate index increased. The hardness, stress at 100% elongation and tensile strength are increased while elongation at break is decreased.

Mottaghi et al., 2012 [27] studied the effect of nano-ZnO and conventional ZnO on crosslink densities of NR/ SBR blends. The various concentrations ranging from 0.5 to 5 pphr of nano-ZnO and conventional ZnO are prepared. They concluded that using nano-ZnO instead of conventional ZnO with the same concentration increases crosslink density and decreases swelling ratios.

Buytaerta and Luob, 2014 [28] studied the rate of bond degradation in the adhesion interface that caused by heat and humidity aging. They used two different coatings of a normal brass-coated steel cord and Cu–Zn–Co ternary alloy coating to make a comparison between them. They found that removal of cobalt salts from compound leads to improve adhesion retention in heat aging conditions, less hysteresis and slow crack growth rate. The new Cu–Zn–Co ternary allows cobalt salts to be removed from tires, which makes the tires more tough and eco-friendly.

2.2 Concluding Remarks

There are numerous forms of rubber compounded and steel tire cord with a different coating. These factors describe the improved pull-out force with and without effect temperature, cure characteristics and other mechanical properties available in the literature.

Most of the works presented in the literature are based on either one of the aforementioned models or modifying these models to establish a new constitutive model. Resulting adhesion between rubber compound and steel tire cord improved by changing the rubber compound, coated steel cord or cure time and cure temperature. A compound of rubber changes by using a different type or percentage of material to get on a compound with optimum pull-out force in steel cord and other mechanical properties.

The most materials that widely considered when investigating its percentage are carbon black, cobalt salt, sulfur and nano-zinc oxide. Some researchers studied the effect of zinc oxide or cobalt content in brass-coated steel cord. All researches didn't consider the effect of nano-ZnO on the pull-out force in steel tire cord. They focused only on the cure characteristics and other mechanical properties.

In this thesis, the study is focused on using nano-ZnO and how to obtain optimal pull-out force with and without effect temperatures on adhesion force that will help to reduce the forming time and cost. In addition, investigations are conducted including hardness and tensile properties.

From this chapter, it is noted that there is a lack of numerical work concerning the wires reinforcing rubber.



CHAPTER THREE
EXPERIMENTAL
WORK

EXPERIMENTAL WORK

3.1 General

In order to acquire a better understanding of the adhesion between rubber compound and steel cord wires, experimental investigations are performed under different conditions. The experimental tests focused mainly on performing adhesion tests, tensile tests and hardness tests on the fabricated specimens. Adhesion tests are carried out under different temperature in order to understand the effect of increasing the temperature on the pull-out force on the adhesion of specimens. The other tests are performed in order to investigate the mechanical properties of rubber compounds.

To understanding the effect of nano-ZnO of reinforcing the rubber with steel wires and temperature effect on the adhesion force is one of the essential goals of this thesis. The final product is the main motivation to do further tests in order to achieve a beneficial recommendation which can be helpful to Babylon factory to manufacture tires with better properties.

The rubber compound doesn't subordinate to constant weight for material, the compound used in a place is not necessary to be used in another place because the tire manufacturing depends on the condition prevailing in the territory, thus Dunlop is not recommended by using standard recipes but is to be established in the territory [17].

3.2 The Used Materials

It is necessary to mix an elastomer with certain additives to improve the properties rubber compounds because each have a specific role either in processing or vulcanization.

All the used ingredients are usually given in amounts created on a total of 100 parts of the rubber and used with a notation, parts per hundred rubber (pphr). Thus, when comparing various recipes, the effects of varying any used ingredient is simply recognized when the physical properties are compared. performance of Product the requirements will order the initial choices of the compounding ingredients [29]. The materials used in the experiments are listed in Table (3.1).

Table 3.1: Type of Materials Used in the Experiments.

Material	Properties
Standard Malaysian rubber (SMR20)	Specific gravity 0.90, volatile matter 0.5% max, Ash 1% max, Nitrogen content 0.5 % max
Zinc oxide	Purity 99 %, Particle size 0.5-1 μ m, Surface area 3-5m ² /g
Nano-zinc oxide	Purity 99%, Particle size < 80nm
Stearic acid	Specific gravity 0.85, Ash at 550 °C 0.1 % Max, volatile matter at 65 °C 0.5% Max
Phenolic tack resin	Specific gravity 1.00-1.05, Ash at 550 °C 0.5% Max
6PPD	Specific gravity 1.00, Melting point 44-50 °C, Ash at 55°C 0.3 % Max, volatile matter at 65°C 0.5 % Max
Carbon black (N-326)	Surface area 77 m ² /g, Pure density 446-470 kg/m ³ , Partical size 26-30 nm
Process oil	Specific gravity 0.87-0.89, Total sulphur 0.5% Max, Ash at 55°C 0.01% Max

Cobalt stearate	Specific gravity 1.09, Ash at 350°C 13.4% Max, volatile matter at 105°C 2% Max
DCBS	Specific gravity 1.3, Ash at 550°C 0.4% Max, volatile matter at 65°C 0.5% Max
Sulfur	Specific gravity 2.10, Ash at 550°C 0.2% Max, volatile matter at 80°C 0.5% Max
CTP-100	Specific gravity 1.3, Ash at 550°C 0.4% Max, volatile matter at 65°C 0.5% Max

3.2.1 Standard Malaysian Rubber (SMR20)

The SMR20 is one type of natural rubber; it is the original of all elastomers. It has been produced mostly in Southeast Asia, especially the countries of Malaysia and Indonesia, this combined produces 80% of the world consumption. It is produced in the form of latex from the bark of the hevea tree [29]. It has a high tensile strength, a very high elasticity, a very good abrasion resistance, a low relative cost and very good dynamic mechanical characteristics. These factors give the natural rubber advantages to be used in tires manufacture [3].

3.2.2 Zinc Oxide

Zinc oxide is the most common activator used in the rubber industry for an increase in quality, efficiency and the vulcanization rate by reducing the time of vulcanization. The zinc cations in zinc oxide react with organic accelerators to form an active zinc-accelerator complex. It is one of the main steps in the vulcanization process to form crosslinks between rubber chains. Traditionally, the addition of conventional ZnO to rubber compound is 3-8 pphr [11].

3.2.3 Nano-Zinc Oxide

The efficiency of ZnO during vulcanization can be increased by maximizing the contact between ZnO particles and the accelerators in the rubber preparation. The average particles size of conventional ZnO is usually in the range 0.3-1.0 μm and its specific surface area is correspondingly in the range 4-6 m^2/g . Nano-ZnO presents high activity due to its small particle size and large surface area. Nano-ZnO has an average particle size less than 100 nm and a specific surface area greater than 15 m^2/g . The equivalent replacement of conventional ZnO by nano-ZnO leads to an improvement of the properties of the rubber compound. This might be due to the fact that the higher specific surface area and therefore a relatively higher amount of Zn^{2+} ions is compared to conventional ZnO. For this reason, a great reduction in the zinc oxide content in rubber compounds is achieved [11].

3.2.4 Carbon Black

Reinforcement of rubber has been defined as the combination of small particles of materials, known as fillers, into elastomer which improves the mechanical properties of the elastomer such as modulus, tensile strength, tear resistance, and abrasion resistance of the final vulcanized rubber. Carbon black is the main reinforcing filler used in rubber compounds to improve durability and strength [3].

3.2.5 Steel Cord

Steel wire used in tires is of various formations. The brass-coated wire strands wrapped together to give cords of various characteristics, depending on the application. Steel tire cord is made from high carbon steel rod, which is first drawn down to a diameter of nearly 1.2 mm. A brass plating is then added to the wire before an ending drawing to 0.15-0.40 mm thickness. These filaments are next stranded to make a cord construction that is planned and optimized for

a specific service requirement. From necessity manufactured steel tire cord from high quality steel because of the performance requests to which tires are subjected. The tire cord construction is defined by the structure, the length and the direction of lay. The description of a steel cord is given by [3]:

The full description of a steel cord = Strand1{(N×F)×D} + Strand2{(N×F)×D} + Strand3{(N×F)×D} + (3.1) [4].

where

N: number of strands

F: number of filaments

D: nominal diameter of filaments (mm).

The steel cord construction used in this work is 2+2×0.28 mm, which means that the cord has two strands and two filaments with 0.28 mm diameter, and this cord coated with brass (Cu/Zn, 64/36) %. As shown in the Figures (3.1) and (3.2).

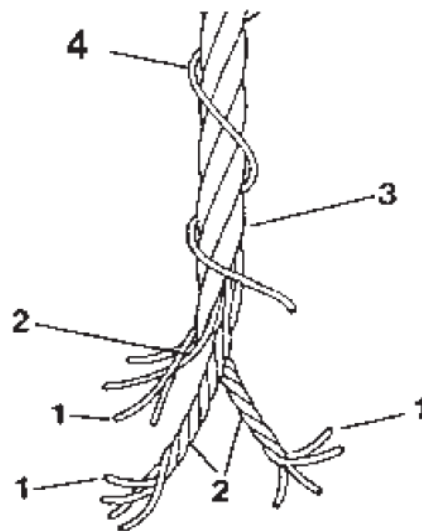


Figure 3.1: Steel Cord Components/ (1) Filament, (2) Strands, (3) Cord, (4) Spiral Warp [4].

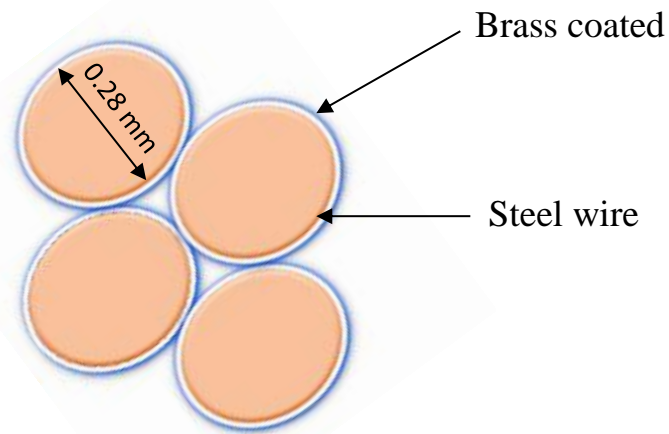


Figure 3.2: The Cross Section of Steel Cord.

3.3 Compounding Recipes

The compounds are classified into four groups depending on the using ZnO, Nano-ZnO, cobalt stearate and carbon black.

1. (A) a standard compound, which is used in State Company for Tire Industry in Najaf, included conventional ZnO as listed in Table (3.2).
2. (B) the group includes the compounds which replaced conventional ZnO in (A) compound with Nano-ZnO as listed in Table (3.3).
3. (C) compound includes the compound which represents change pphr of cobalt stearate in best compound of (B) group as listed in Table (3.4).
4. (D) compound includes the compound which represents change pphr of carbon black in best compound of (B) group as listed in Table (3.5).

The weight of natural rubber SMR20 equals to 200 grams in any compound so that the ratio of the weight of total rubber in grams and in pphr equals to 2:1.

According to the above recipes, the weight of any ingredient can be calculated as follows:

The weight of ingredient (grams) = 2 × the weight of ingredient (pphr)... (3-2)

Table 3.2: Rubber Compound Recipe of (A) in pphr.

Material	A
SMR20	100
Zinc oxide	8
Nano zinc oxide	0
Stearic acid	1.4
6PPD	1
Phenol tack resin	0.8
Carbone black	50
Oil process	7.7
Cobalt stearate	1
DCBS	0.7
Sulfur	4.5
CTP- 100	0.4

Table 3.3: Rubber Compound Recipe of (B) in pphr.

Material	B1	B2	B3	B4	B5	B6	B7	B8
SMR20	100	100	100	100	100	100	100	100
Zinc oxide	0	0	0	0	0	0	0	0
Nano zinc oxide	0.2	0.6	1	1.4	1.8	2.2	2.75	4
Stearic acid	1.4	1.4	1.4	1.4	1.4	1.4	1.4	1.4
6PPD	1	1	1	1	1	1	1	1
Phenol tack resin	0.8	0.8	0.8	0.8	0.8	0.8	0.8	0.8
Carbone black	50	50	50	50	50	50	50	50
Oil process	7.7	7.7	7.7	7.7	7.7	7.7	7.7	7.7
Cobalt stearate	1	1	1	1	1	1	1	1
DCBS	0.7	0.7	0.7	0.7	0.7	0.7	0.7	0.7
Sulfur	4.5	4.5	4.5	4.5	4.5	4.5	4.5	4.5
CTP- 100	0.4	0.4	0.4	0.4	0.4	0.4	0.4	0.4

Table 3.4: Rubber Compound Recipe of (C) in pphr.

Material	C
SMR20	100
Zinc oxide	0
Nano zinc oxide	2.2
Stearic acid	1.4
6PPD	1
Phenol tack resin	0.8
Carbone black	50
Oil process	7.7
Cobalt stearate	2
DCBS	0.7
Sulfur	4.5
CTP- 100	0.4

Table 3.5: Rubber Compound Recipe of (D) in pphr.

Material	D
SMR20	100
Zinc oxide	0
Nano zinc oxide	2.2
Stearic acid	1.4
6PPD	1
Phenol tack resin	0.8
Carbone black	65
Oil process	7.7
Cobalt stearate	1
DCBS	0.7
Sulfur	4.5
CTP- 100	0.4

3.4 Preparing and Mixing Compound Materials

The materials used in this work are weighing by using the laboratory balance establishing a balance with ± 0.001 -g accuracy. It is carried out according to ASTM D3182.

The mixing process accomplished in State Company for Tire Industry in Najaf, is according to ASTM D3182 [30]. The specific weight of each material is mixed by two-roll laboratory mill (300×150 mm) with 0.5 kg capacity as shown in Figure (3.3). The rolls mill are made of steel with a hardened surface. They typically apply a high pressure to produce a thin sheet of rubber.



Figure 3.3: Rolls Mill.

The process of mixing starts by putting natural rubber SMR20 between the rolls and additive other materials mix on two-roll laboratory mill. The process is repeated many times until the whole material has got well masticated. The ingredients are added as follows:

1. The SMR20 is masticated in two roll mills several times with decreasing the distance between the rolls at a constant temperature at of 70 °C.

2. The ZnO is added to the SMR20 and then follows the same procedure in step 1.
3. The following additives are added to the mixture of SMR20 and ZnO in consequence and then follows the same procedure in step 1. These additives are stearic acid, 6PPD, cobalt stearate and phenol tack resin.
4. Mixing a half of carbon black 25 pphr with oil and then adding them to the homogeneous materials following the same procedure in step 1.
5. Adding the other half of carbon black alone and finally adding sulfur, DCBS and CTP-100 and following the same procedure in step 1.

It is important to mention that the total mixing time is kept to a minimum in order to avoid sticking of the rubber compound to the mill rolls. Table (3.6) shows the time for all process.

Table 3.6: Mixing Schedule.

NO	Operations	Time (minutes)
1	Mastication of SMR20 rubber	4
2	Addition of zinc oxide	2
3	Stearic acid, 6PPD, cobalt stearate, phenol tack resin	2
4	Addition of carbon black + oil	6
5	Addition of carbon black	4
6	Sulfur, CBS, CTP-100	4
7	Sweep and dumb	3
8	Total	25

3.5 The Fabrication Specimen and Testing Work

3.5.1 Vulcanization Rubber Specimen

In this work the vulcanization process of the rubber compound is started by heating the thermal hydraulic press which is used in vulcanization process. It is carried out in the State Company for Tire Industry and according to ASTM D3182 [30].

The press is heated by a hydraulic power unit which consists of two jaws used to generate a high pressure on the mold as shown in Figure (3.4). The maximum pressure of the press is 4 Mpa, press dimensions are 457 x457 mm, closing speed is approximately 200 mm/minute and the range of temperature is 0-200 °C [31].



Figure 3.4: Thermal Hydraulic Press.

3.5.2 Hardness Test

The mold of hardness test has dimension $200 \times 180 \times 6.5$ mm with nine holes; each hole has 45 mm diameter and 5 mm thickness. The test piece puts inside the holes. The vulcanization process is started by selecting the temperature at 175°C and the pressure of the press at 3.5 MPa on the cavity during vulcanization [32]. The empty mold is put between the jaws at least for 20 min before inserting unvulcanized pieces. The press is opened and the unvulcanized pieces are inserted into the mold. The mold is put between the jaws and pressed for 15 min to produce the hardness disc as shown in Figure (3.5).

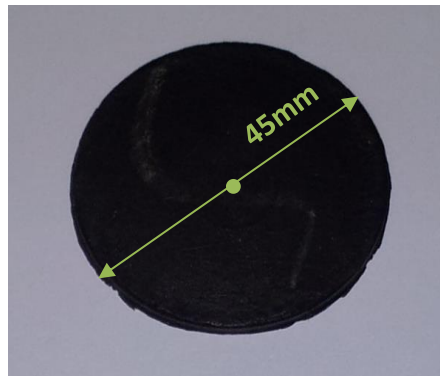


Figure 3.5: Hardness Disc.

In hardness test, the Wallace Dead Load Hardness Tester is used as shown in Figure (3.6). This device is manufactured by Wallas Startorius GMBA CO., Gottingen, England. The hardness of rubber is measured by penetration process. Readings are donated directly in IRHD which is the international rubber scale.

The test is based on the measurement of the notch of a rigid ball into the rubber under specified conditions. The test is carried out at $25 \pm 2^\circ\text{C}$, it is placed on the bottom table of the device and must have a flat surface, smooth and

paralleled edges surface. The working wheel is turned by hand to rest on the surface of the test sample. The value of the hardness is recorded on the gage in IRHD and taking the average value of the three different points distributed over the test sample.

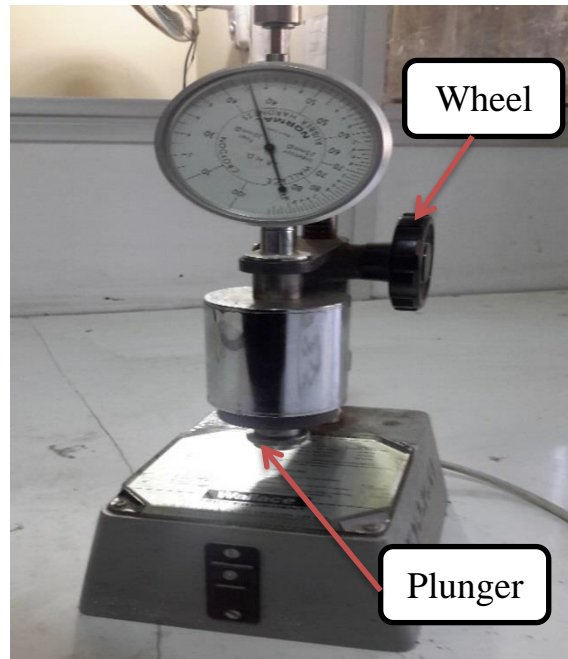


Figure 3.6: Dead load hardness tester.

3.5.3 Tensile Test

Vulcanization process of the previously mentioned rubber compounds is started by selecting the temperature at 150°C and the pressure at 3.5 MPa of the thermal hydraulic press [32]. The mold of tensile test has two cavities with dimensions 150×150×2 mm which is filled with 70 gram from the compound recipe. The mold is put between the jaws and pressed for 45 min to produce a thin sheet of rubber which can be used later to make the dumbbell specimens. The vulcanized thin rubber sheet shown in Figure (3.7), it is released from the mold and left to cool down in room temperature for a sufficient period of time.

Finally, by using the cutter (Wallace) shown in Figure (3.8) the dumbbell specimens of a tensile test are obtained under ASTM D412 specifications as shown in Figure (3.9). The cutter is manufactured by Wallas Startorius GMBA CO., Gottingen, England manufactured. The press contains a ram which moves vertically under the control of a lever, it is motivated with one hand by the operator. The lever is counterbalanced by a weight [31].

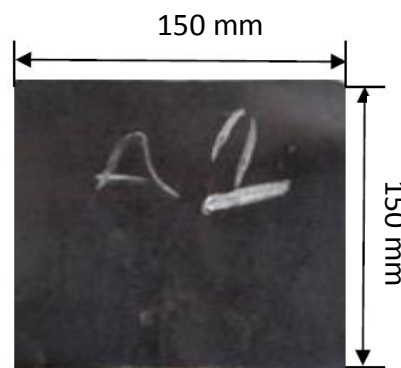


Figure 3.7: Tensile Sheet.



Figure 3.8: Specimen Cutting Press.

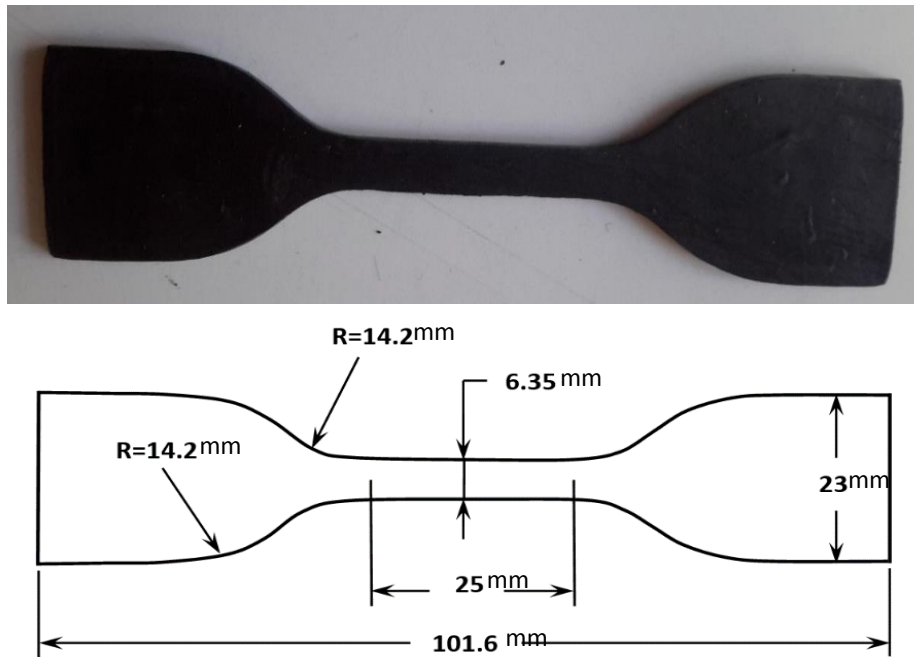


Figure 3.9: Dumbbell Specimen of Tensile Test.

To start the test, the Monsanto T10 Tensometer device is used as shown in Figure (3.10). It is manufactured by Monsanto CO., England. The important specifications of Tensometer are range of force: 1-10 KN, crosshead speed range: 0.5-1000 mm/min, and range of strain: 0.1-5000 % [31].

The data entered on the control board of Tensometer is the speed of moving grip 500 mm/min and thickness of dumbbell which is measured by micrometer which has range 0-25 mm. The tensometer consists of upper and lower gripes which are used to hold both ends of the tensile samples under consideration. When a device is operated, the above grip raised, the dumbbell lengthened and broke down. The results recorded are the elongation, tensile strength, and modulus at 100%, 200%, 300% by the printer, which is connected with the tensometer. Three more dumbbells from the same sheet are tested in order to take the average value of the three results.

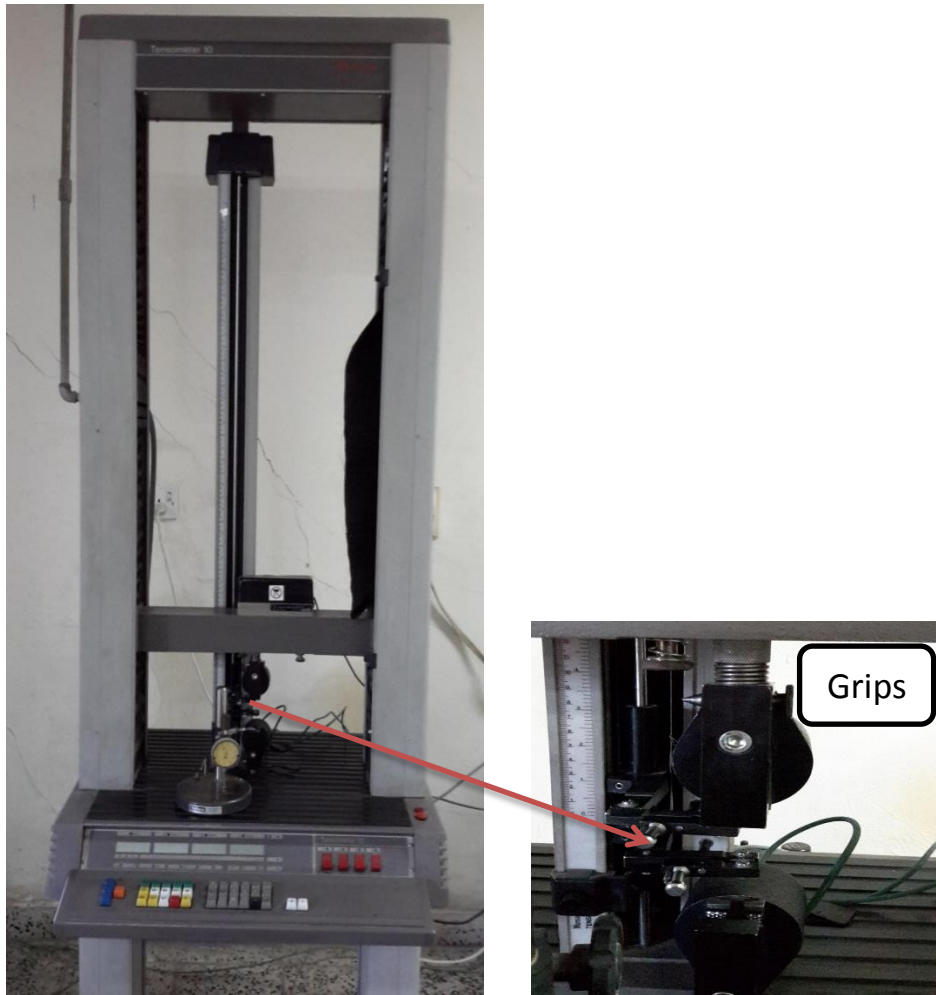


Figure 3.10: Monsanto T10 Tensometer.

3.5.4 Adhesion Test

To get an adhesion sample using the mold which has three parts; base die, cover die and steel die. Base die and cover die have similar dimensions $300 \times 150 \times 5$ mm while the dimension of steel die is $300 \times 115 \times 12.5$ mm. The steel die has a hole with dimension $200 \times 12.5 \times 12.5$ mm for inserting the unvulcanized pieces inside the hole and 15 grooves for inserting the steel wire inside grooves, as shown in Figure (3.11). The vulcanization process is started by selecting the temperature at 145°C and the pressure of the press at 3.5 MPa [32]. To get adhesion sample cutting the unvulcanized piece into two parts with same dimensions and inserted into the hole, put wires in grooves to embed into

the piece then put another piece on the first, and the press is closed in the possible minimum time. The mold is put between the jaws and pressed for 30 min to produce a T- adhesion sample. Finally, these samples are must be cleaned after vulcanization by the cutter to cut wires from one side and then used codes to remove external rubber from wires in another side, Figure (3.12) shows the final shape of adhesion specimen.

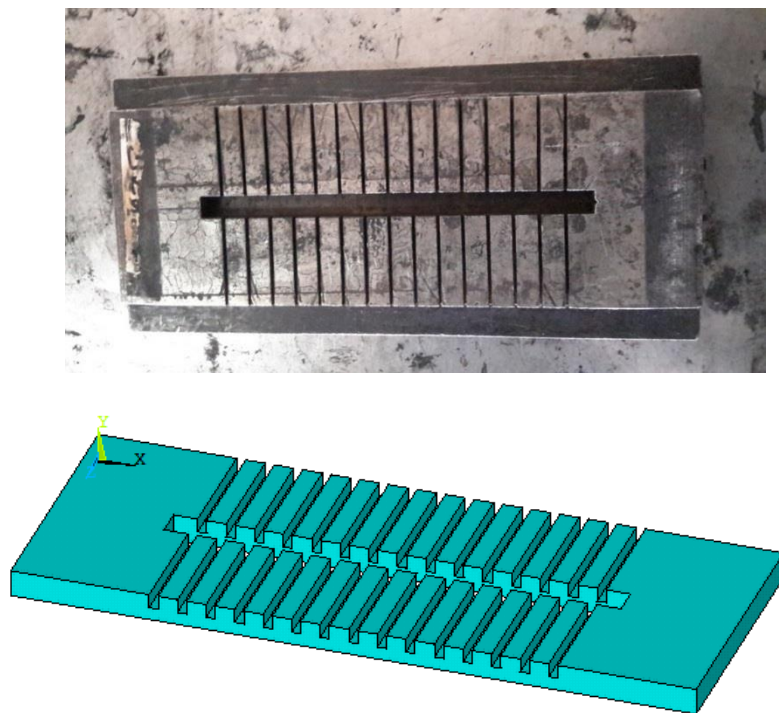


Figure 3.11: Mold of Adhesion Sample.

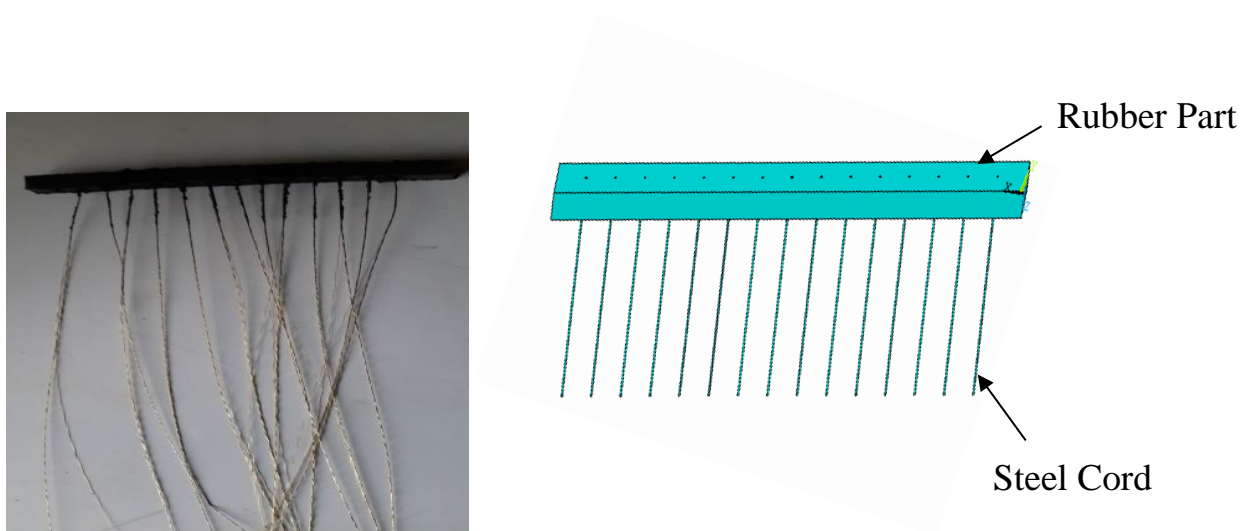


Figure 3.12: Adhesion Specimen after Cleaning.

To start the test, the Monsanto T10 Tensometer device is used by changing the grips of a tensile test to shoulder grip according to ASTM D2229-cord pull on tire compound as shown in Figure (3.13) [33].

The T- adhesion sample is placed in two grips of the tensometer, the vulcanized rubber block is placed with the upper grip and the free wire is caught in the lower grip. The speed of moving grip is fixed at 100 mm/min, and a value of 1000 N force is entered into the controller board of tensometer. When the device is operated, the steel cord pulls out from a block of vulcanized rubber and the result of force is recorded by the printer. All cords are tested and then the average value of the force was taken for wires. To produce the adhesion test with different temperature put sample in oven. The oven works with a range of temperature 0-200 °C. Open the oven and set the temperature at 50 °C, the second sample is inserted into the oven then measure the temperature of the sample with a thermometer, when it reaches 50 °C; translate the sample to the Tensometer to measure the pull-out force. Set temperature of the oven at 75 °C to insert the third sample and then set the temperature at 100 °C to insert the fourth sample then do the same procedure of the second sample. Four T-adhesion samples for any compound are tested and then find the average value of the pull-out force results.

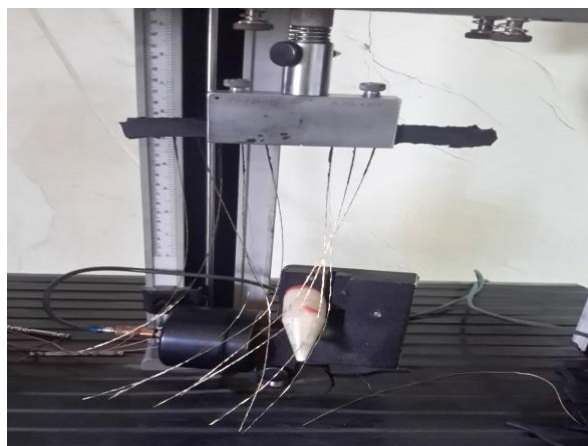


Figure 3.13: Grips of Adhesion Specimen.



CHAPTER FOUR
NUMERICAL WORK

NUMERICAL WORK

4.1 General

In this chapter, the numerical procedure of the present work is discussed and the finite element simulation procedure is used to evaluate pull-out force in steel wire.

4.2 Finite Element Method

The finite element method (FEM) is a numerical technic method for solving different mechanical problems, which are typically as well complex to be solved analytically. The FEM can also be used to calculate equivalent composite properties from a model where the geometry of the cords and rubber is explicitly represented.

The linear composite analysis combined with nonlinear finite element analysis can give a reasonable description of the material response for most applications. FEM that allows the cord and rubber properties to be specified separately, rather than smeared into composite coefficients, can provide a very powerful method to represent the nonlinear response of cord-rubber composites [4].

4.3 Finite Element Software Package ANSYS 16.1

The method to use ANSYS graphical user interface (GUI) follows the conventions of common Windows. The input data for an ANSYS analysis are prepared using a preprocessor. The preprocessor (defining the problem) is used to define the element types, element real constants, material properties and the model geometry [34].

The important stages of developing the FE solution are:

- Defining problem type, the problem type in this work is structure.
- Defining element type.
- Defining material properties.
- Draw model geometry.
- Mesh generation.
- Create of contact.
- Applying a load and boundary condition.
- Selection of the appropriate solution method.

4.3.1 Defining Element Type

The ANSYS element library contains more than hundred different element types [34]. In the current study, the elements used is solid brick 8 nodes 185 as shown in Figure (4.1). This element is used for 3D modeling of solid structures. It is defined by eight nodes having three degrees of freedom at each node, translations in the x, y and z directions. It has plasticity, hyperelasticity, creep, stress stiffening, large deflection, and large strain capabilities. The element also has the mixed formulation ability for simulating deformations of nearly incompressible elastoplastic materials, and fully incompressible hyperelastic materials.

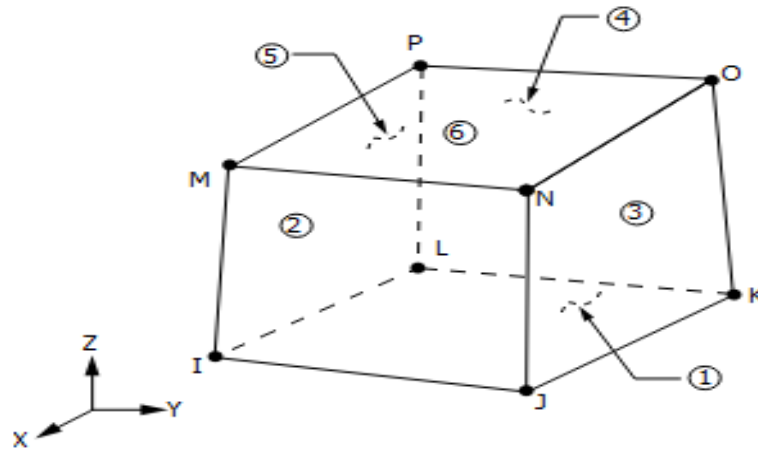


Figure 4.1: SOLID185 Homogeneous Structural Solid Geometry.

4.3.2 Defining Material Properties

Material properties are required for most element types. Depending on the application, set of material properties may be linear or nonlinear, isotropic, orthotropic or anisotropic, constant temperature or temperature dependent [34]. In this study the material is defined by nonlinear and then input properties as the following:

- Define the elastic behavior of uniaxial tensile test data from experimental work for rubber block material listed in the appendix-A, this property is used the Mooney-Rivlin to describe the behavior of the rubber.
- The steel material is used as a rigid body to build the finite element model.

4.3.3 Draw Model Geometry

There are two ways to draw the finite-element model in ANSYS: solid modeling and direct generation. With solid modeling, the geometry of the model is described, and then the package ANSYS automatically meshes the geometry with nodes and elements, which can be controlled by the size and shape of the elements. With direct generation, the place of each node and the connectivity of each element is manually defined. Several convenience processes are available, such as add, delete and overlap [34]. The second method is preferred especially with complex geometry and was used in the present study. The 3D model is shown in Figure (4.2) with $25 \times 12.5 \times 12.5$ mm dimensions, which is a section from rubber block with one wire in experimental work.

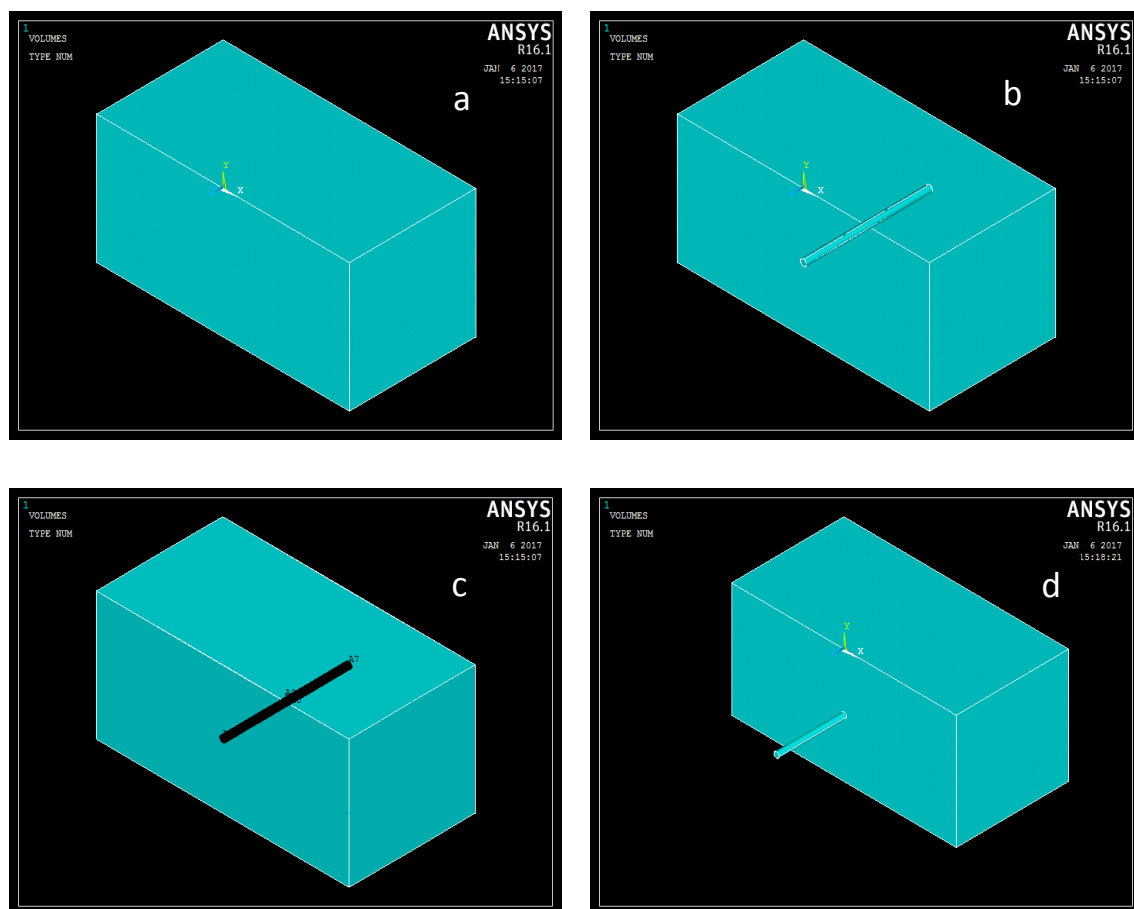


Figure 4.2: The Parts in 3D Model of Rubber Block and Steel Cord.

4.3.4 Mesh Generation

The meshing stage is an important step by which the geometric model is transformed into the finite element model. The mesh generation for a geometrical model is processed by controlling the length and volume of elements. Figure (4.3) shows the model after meshing. The numerical tests have been done to get the best number of elements by using mesh tool and a number of elements used 3D simulation process to attain the steady state solution. The best number of elements are 1899 element as shown in Figure (4.4).

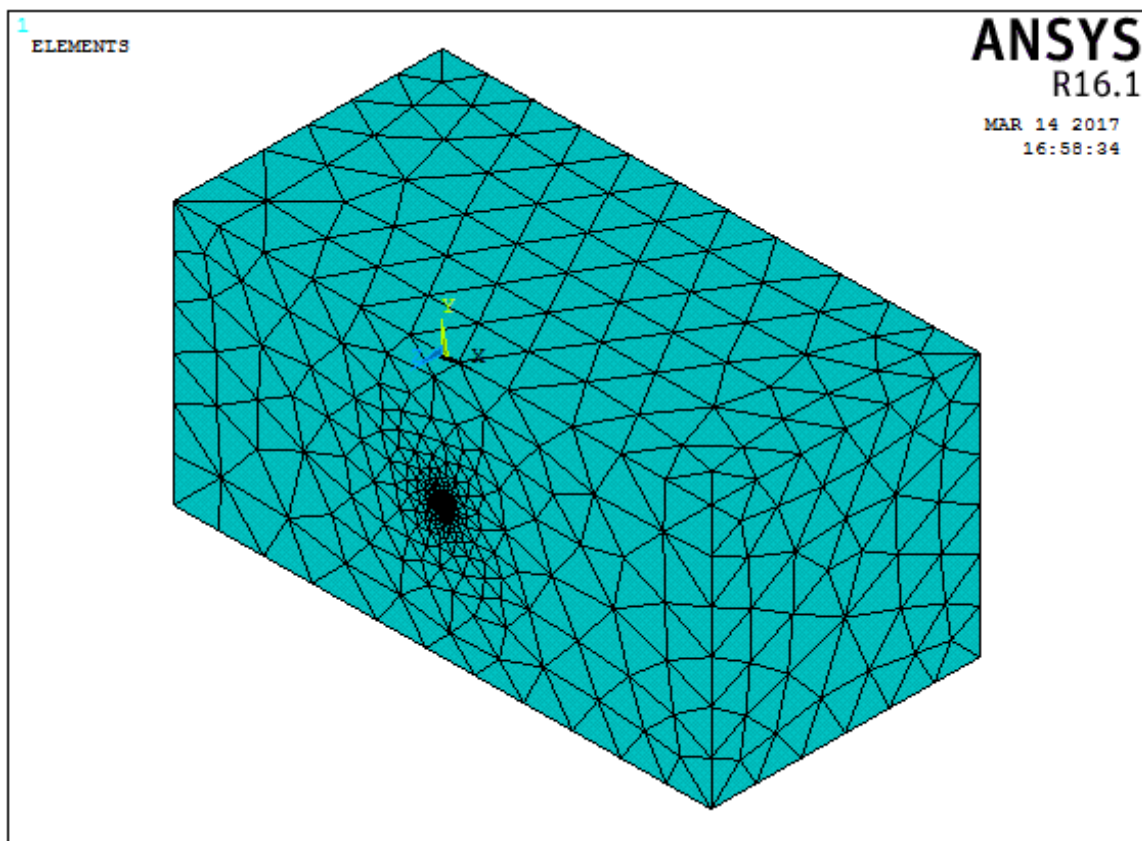


Figure 4.3: Mesh Generation for Rubber Block.

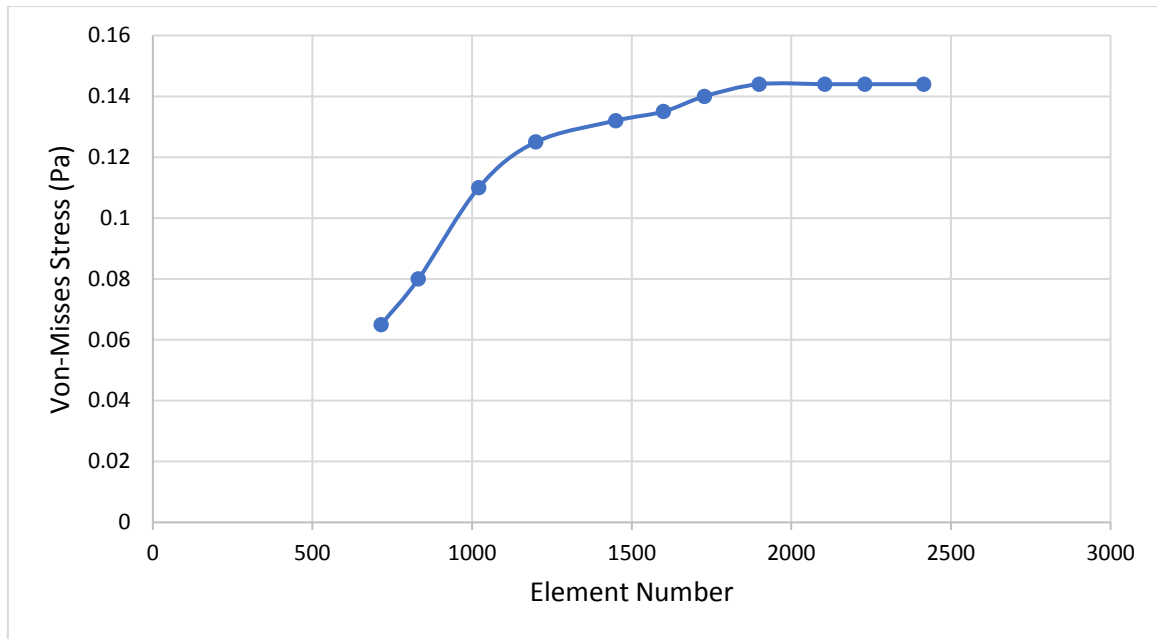


Figure 4.4: Relationship Between Number of Element and Von-Misses Stress on Rubber Block.

4.3.5 Create of Contact

The contact and target surfaces comprise a “Contact Pair”. In the current study, contact pairs are constructed between rubber block and steel wire. A contact pair with rigid target creates one pilot node to govern the motion of the target surface. The pilot node can be one of the nodes one the target elements or a node at any arbitrary location. For each pilot node, the program automatically defines an internal node and an internal constraint equation. The types of contact are node to node element, node to surface element and surface to surface element. The type of the contact in this study is surface to surface element. It is well- suited for applications such as interference fit assembly contact or entry contact, forging and deep drawing problems. These elements are the most widely used contact elements in ANSYS, due to the many advantages that they are compatible robust, feature-rich and user friendly.

To represent contact and sliding between the target surface and a deformable surface, the CONTA174 is used as shown in Figure (4.5). The element is suitable for 3D structural and coupled field contact analyses. The location of this element is on the surfaces of 3D solid or shell elements without mid-side nodes. It has the same geometric characteristics like the solid or a shell element which is a face that is connected with. Contact has occurred when the element surface penetrates one of the target segment elements TARGE170 on a specific target surface.

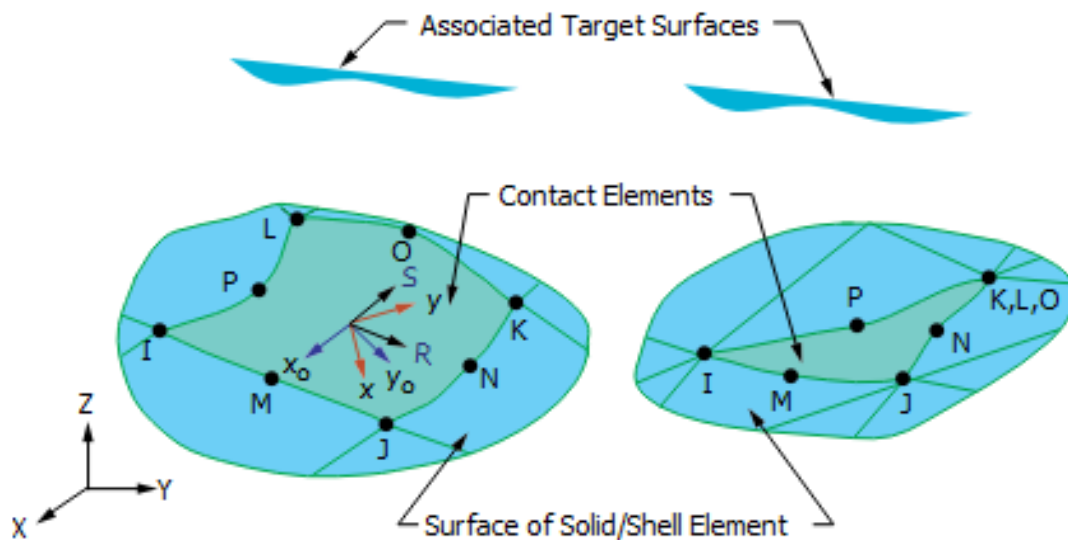


Figure 4.5: CONTA174 Geometry.

TARGE170 is used to represent various 3D "target" surfaces of the associated contact element CONTA174 as shown in Figure (4.6). The contact elements themselves overlay the solid, shell, or line elements and this describes the boundary of a deformable body and those which are potentially in contact with the target surface, defined by TARGE170. This target surface is discretized by a set of target segment elements TARGE170 and is paired with its associated contact surface via a shared real constant set.

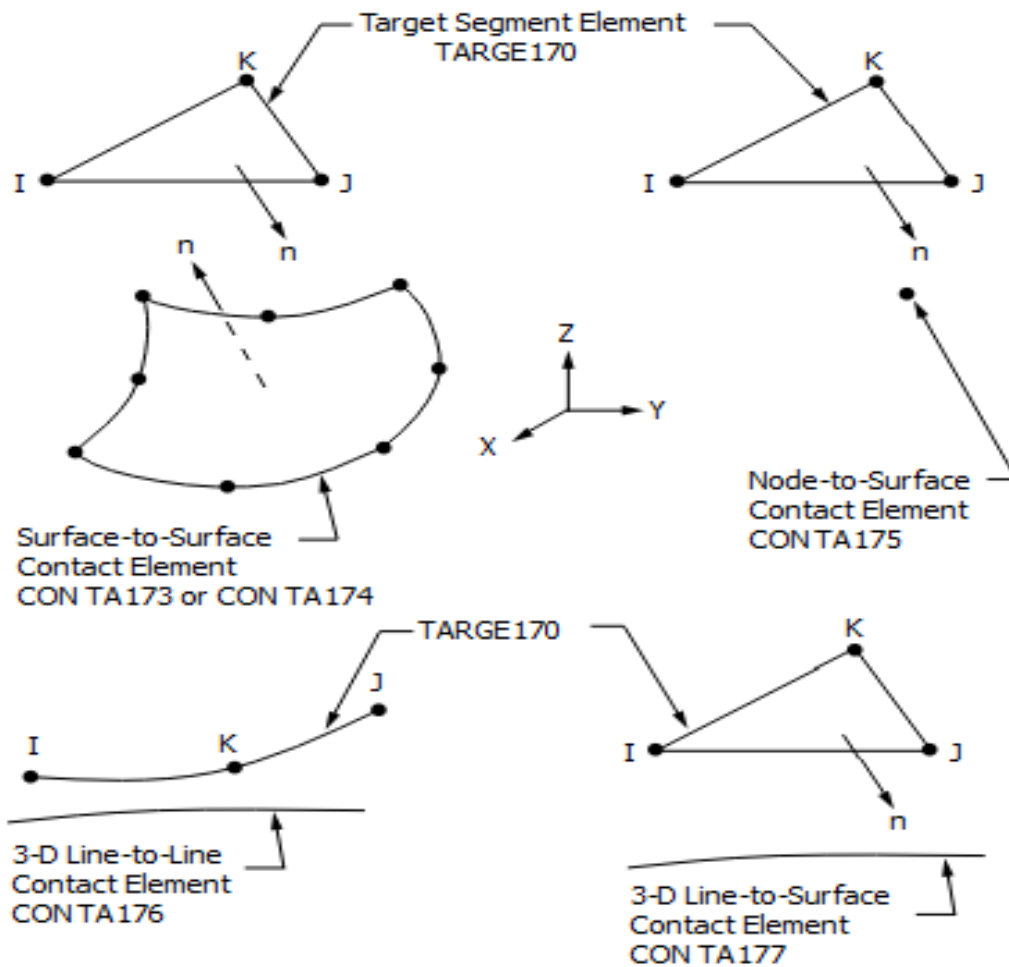


Figure 4.6 TARGE170 Geometry.

4.3.6 Applying a Load and Boundary Condition

The load and boundary conditions in this study are applied by using the solution processor with defining boundary condition. This can be defined by applying zero displacements on all degrees of freedom nodes of six surface in rubber block. The load in steel cord is also applied by using the solution processor with load step options. This can be defined by applying a range of force in the positive Z-direction of a pilot node and then starts the finite element solution, as shown in Figure (4.7).

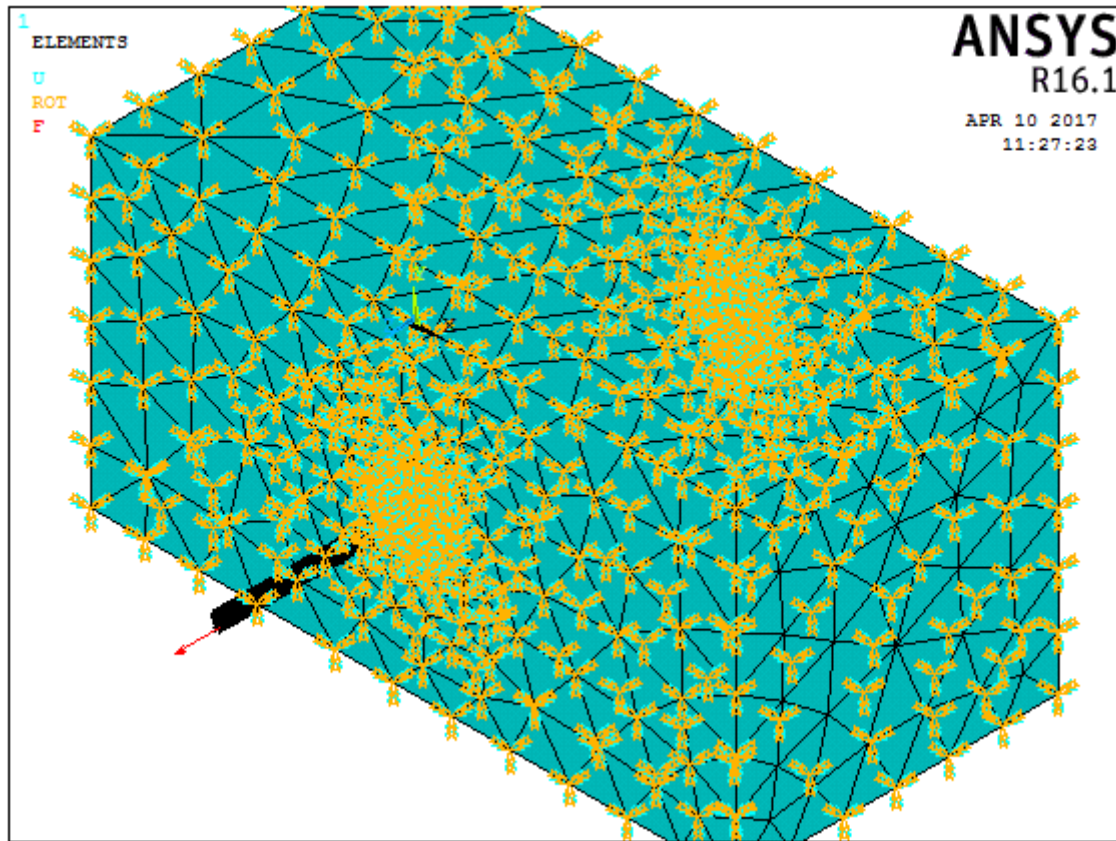
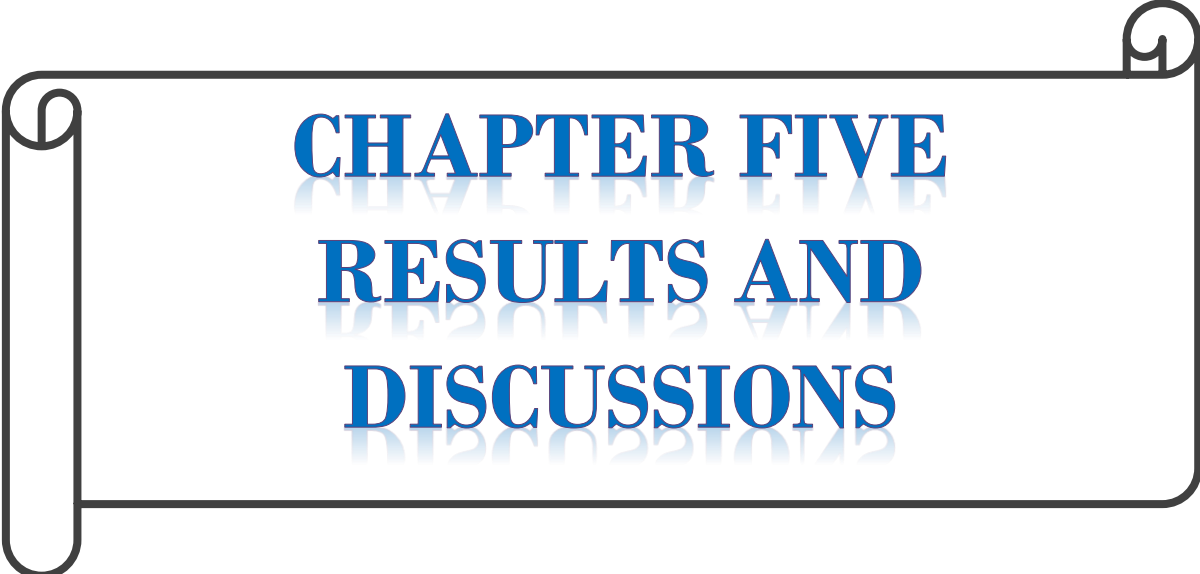


Figure 4.7: Define load and Boundary Condition.



CHAPTER FIVE
RESULTS AND
DISCUSSIONS

RESULTS AND DISCUSSION

5.1 General

This chapter consists primarily of two sections. The first one concerns with the identification of material parameters based on the experimental tests of the present study. In this section, the interest of the work focuses on identifying the effect of nano-ZnO and increased temperature on the pull-out force in steel tire cord on the adhesion samples. Moreover, the cure characteristic test, tensile test, and hardness test is studying to recognize the efficiency of the compounds.

The second section of this chapter concerns with performing finite element method. The finite element model is constructed to match the geometry and physical properties of the adhesion samples. The processes are achieved by using finite element package ANSYS ver. 16.1. The revealed results are compared to that obtained from the experimental work to verify the accuracy of the suggested model.

5.2 Experimental Part

Through this part, the results of cure characteristics, tensile properties, hardness, and adhesion force with temperature effect are presented and discussed in order to select the maximum adhesion between rubber and steel wires in the best rubber recipe.

5.2.1 Adhesion

The effect of temperature on adhesion is studied. Table (5.1) summarizes the values of T-pull test to get the average force in all cords in (A) compound at 25,50,75,100 °C temperatures. These results are presented in Figure (5.1). As shown, when the temperature increases, the adhesion decreases due to a destructive effect of hot environment on the interfacial interactions of the system. The increased temperature is the main reason of bond breakage at the interface and re-bonding happens when temperature decreases [19].

Table 5.1: Pull-Out Force Values at Different Temperature of (A) Compound.

Compound Sample	A			
Temperature (°C)	25	50	75	100
Pull-out Force (N)	280.64	221.072	213.04	202.8

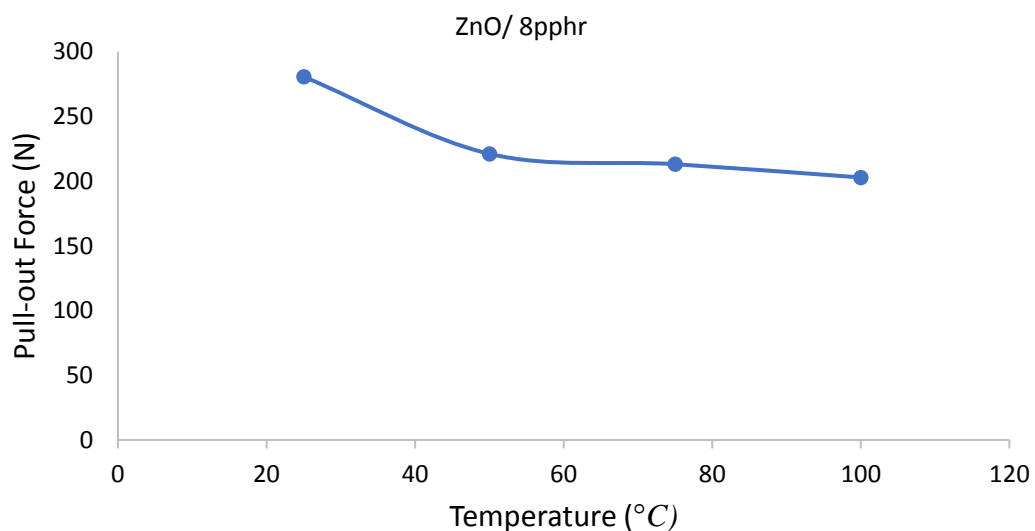


Figure 5.1: Pull-Out Force of (A) Compound at Different Temperatures.

All aging processes lead to a decrease in the amount of S at the interface CuS, as well as, increases in an amount of ZnO and ZnS and this is a key factor for degradation of adhesion. The ZnO is one factor for degradation due to the zinc ions are degrading rubber crosslink and breaking sulphur ring. In order to reduce this factor, conventional ZnO is replaced by nano-ZnO in rubber compound because the nano-ZnO has a smaller particle size and a large surface area than conventional ZnO.

The results of the T-pull test to get the average force in all cords in (B) compounds are summarized in Table (5.2) and presented in Figure (5.2). As shown that an increase in a nano-ZnO leads to increase the pull-out force as well as a low loading of nano-ZnO is not effective for adhesion because of the efficiency of cross-linking system decreases according to the role of used as an activator ZnO in rubber vulcanization [35]. However, loading with 2.2 pphr of nano-ZnO at (B6) compound has optimum pull-out force then it starts to decrease with a loading higher than 2.2 pphr because increasing the amount of ZnO leads to increase the Zn^{2+} ions and these ions degrade the adhesion interface. Also, it is seen that an increase in temperature leads to decrease adhesion in all cases.

Table 5.2: Pull-Out Force Values at Different Temperature of (B) Compounds.

Temperature (°C)		Pull-out Force (N)			
		25	50	75	100
Compound Sample	B1	142.856	126.7	102.32	76.736
	B2	185.063	166.857	154.78	130.725
	B3	231.59	211.978	190.56	170.6
	B4	250.66	219.75	204.01	200.36
	B5	265.26	221.21	217.056	211.25
	B6	297.72	259.5	237.32	233.311
	B7	215.756	203.91	198.23	187.267
	B8	210.37	192.7	189.204	175.581

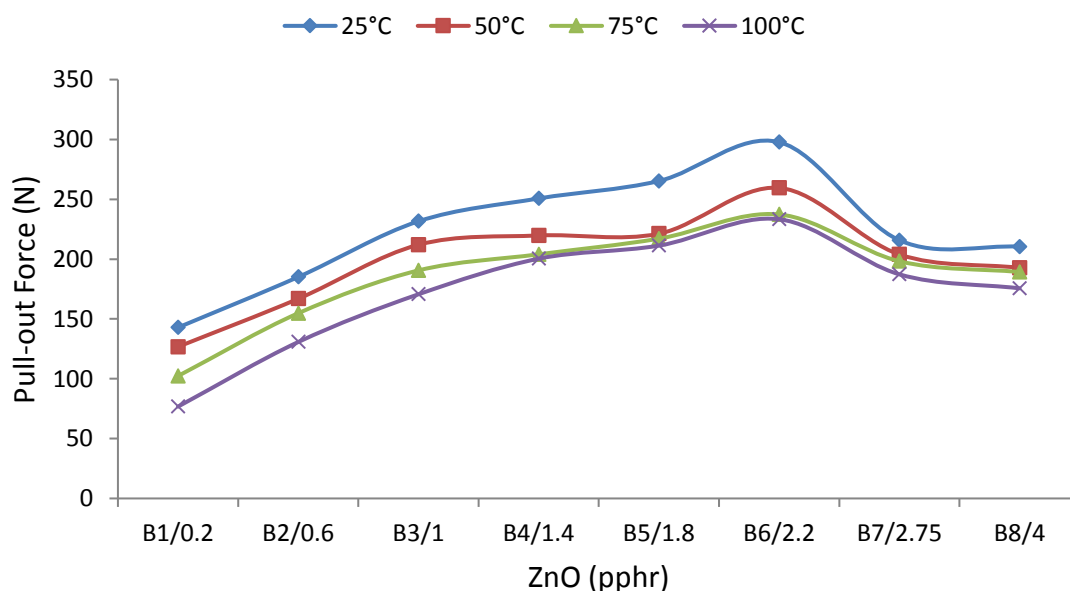


Figure 5.2: Pull-Out Force of (B) Compounds at Different Temperatures.

To show the effect of nano-ZnO on adhesion, the comparison between (B6) (is the best compound in group B compounds) and (A) compound (is used as a standard in State Company for Tire Industry in Najaf) are made. The result of this comparison is that the pull-out force in (B6) compound is greater than (A) compound in all ranges of temperature as shown in Figure (5.3). This is because the Zn^{2+} ions in B6 compound are less than that in (A) compound and this leads to decrease the degradation at the interface and improve the pull-out force by 12%.

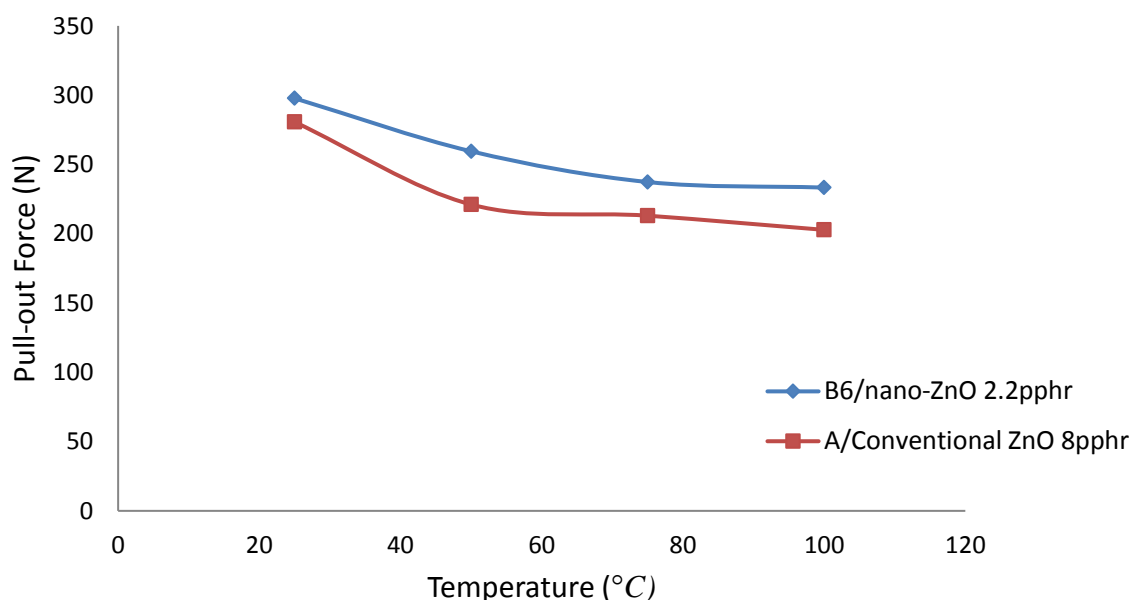


Figure 5.3: Pull-Out Force of (B6) Compound and (A) Compound at Different Temperatures.

According to the role of cobalt in the bonding between rubber and brass prevention of adhesion degradation due to cobalt ions Co^{2+} reducing the conductivity of the ZnO. The effect of cobalt stearate on adhesion bonding was studied by changing the percentage from 1 pphr to 2 pphr [36] in (B6) compound (is the best compound in group B compounds) and then compared the new compound with other compounds. From Figure (5.4), the increasing of

cobalt stearate to 2 pphr shows poor adhesion properties in all temperatures compared to 1 pphr. Increase loading of cobalt stearate causes cracks in rubber compound which leads to easily pull cord. The percentage of cobalt stearate in the rubber compound acts as an adhesion interphase stabilizer in various hostile environments.

Table 5.3: Pull-Out Force Values at Different Temperature of (C) Compound.

Compound Sample	C			
Temperature (°C)	25	50	75	100
Pull-out Force (N)	267.8	233.24	227.04	221.83

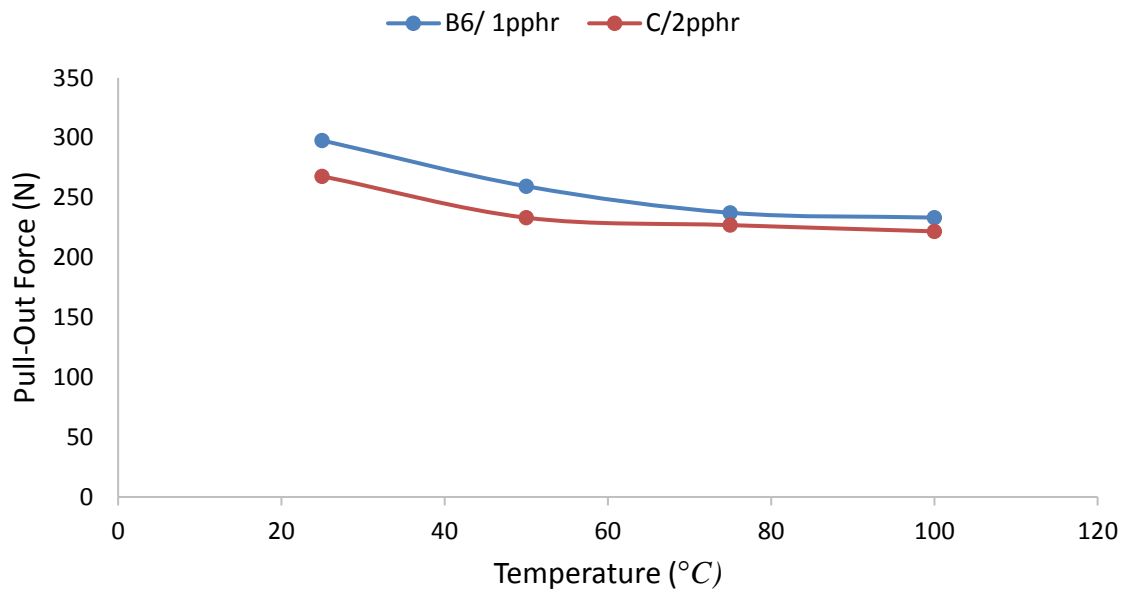


Figure 5.4: Pull-Out Force of (B6) Compound and (C) Compound at Different Temperatures.

5.2.2 Hardness

The effect of nano-ZnO level on the hardness of the compounds is shown in Table (5.4) and Figure (5.5). The results show that hardness increases with increasing nano-ZnO level due to increasing crosslink efficiency and crosslink density.

When the use of nano-ZnO in (B) compound and conventional ZnO in (A) compound in the sulfur vulcanization of the rubbers are compared, the hardness in (B6) compound is 55 IRHD at 2.2 pphr nano-ZnO which is less than the hardness in (A) compound which is 60 IRHD at 8 pphr conventional ZnO. In other words, the crosslink density in (A) compound is greater than that in (B6) compound. Also, according to the results summarized in the same table and presented in Figure (5.6), the hardness in (C) compound is 54 IRHD and it is less than hardness in (B6) compound because it has low crosslink density.

Table 5.4: Results of Hardness Test of (B) Compounds.

Compound Sample	Hardness Rate (IRHD)
A	60
B1	41.33
B2	49.33
B3	49.92
B4	50.667
B5	52.167
B6	55
B7	48
B8	51.5
C	54

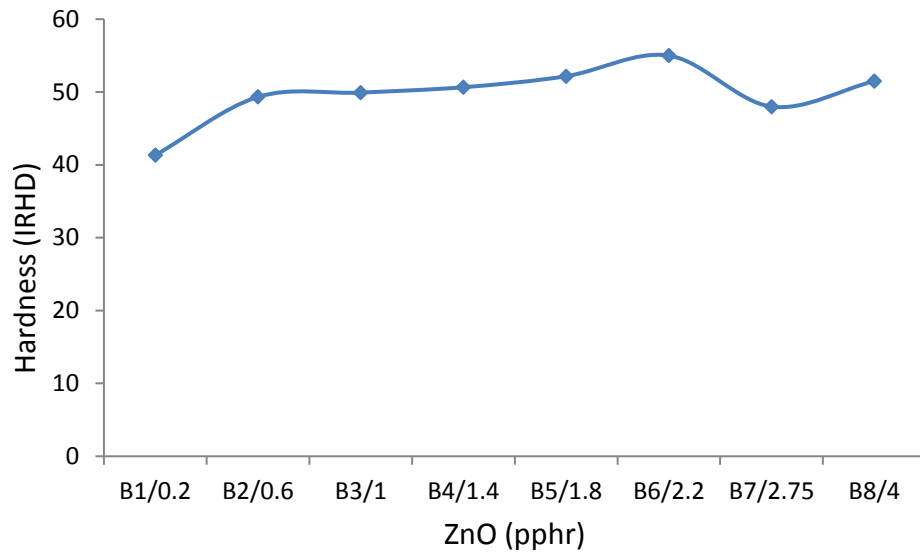


Figure 5.5: Hardness Rate of (B) Compounds.

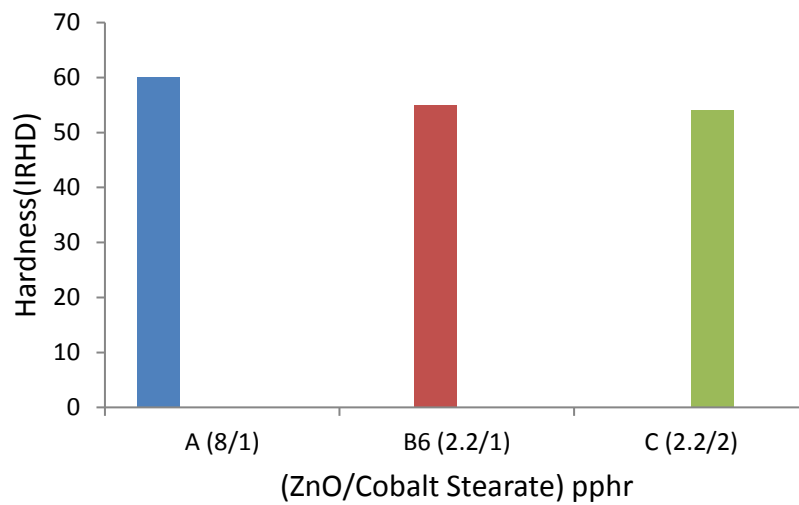


Figure 5.6: Hardness Rate of (A), (B6) and (C) Compounds

5.2.4 Tensile Properties

5.2.4.1 Tensile Strength

According to Table (5.5) and Figure (5.7), tensile strength increases progressively with increasing nano-ZnO level from 0.2 pphr up to a maximum value at 1.8 pphr. This observation is attributed to the consolidation of a network structure of the rubber chains with increasing ZnO level due to increasing crosslink density. But tensile strength decreases with increasing the concentration of nano-ZnO beyond 1.8 pphr due to the relation between ZnO and crosslink density. The crosslink density is proportional to the concentration of ZnO. When the crosslink density increases, the elastomer becomes more elastic and the tensile strength increases and reaches the maximum level as crosslink density at 1.8pphr. When the crosslink density increases after 1.8 pphr, the motion of rubber chains becomes restricted and the tight network is unable to dissipate much more energy.

When the tensile strength for the (B6) compound and (A) compound are compared as shown in Figure (5.8), the average tensile strength for (B6) compound is 13.475 MPa at 2.2 pphr nano-ZnO and it is greater than tensile strength for (A) compound that is 12.602 MPa at 8 pphr conventional ZnO. In this case using nano-ZnO instead of conventional ZnO reduces the amount of ZnO inside the compounds by 72.5% and improves tensile strength by 7%. Also, from the same figure, the (C) compound has a tensile strength less than (B6) compound because crosslink density for (C) compound is less than that for (B6) compound.

Table 5.5: Results of Tensile Test (A), (B) and (C) Compounds.

Compound	Tensile Strength (MPa)	Tensile Strength average (MPa)	Elongation at Break %	Elongation at Break Rate %	Modulus at 300% (MPa)	Modulus at 300% average (MPa)
A	12.238 12.988 12.582	12.602	336 374 297	336	11.256 10.312 8.006	9.858
B1	8.509 7.164 6.606	7.426	603 619 577	600	3.223 3.037 3.496	3.252
B2	10.146 9.929 10.488	10.187	512 460 469	495	3.847 3.863 3.383	3.697
B3	13.365 11.507 12.824	12.565	521 473 491	480	5.5 5.766 5.82	5.659
B4	14.559 13.095 14.899	14.184	526 483 521	454	6.526 6.658 6.687	6.623
B5	20.254 20.451 20.254	20.318	480 428 441	449	10.88 11.996 10.43	11.102
B6	12.984 13.687 13.750	13.475	444 424 432	433	9.387 8.957 8.795	9.046
B7	13.52 12.82 13.311	13.217	482 414 465	445	9.266 8.573 8.295	8.711
B8	13.412 12.915 13.28	13.202	453 377 490	460	7.742 7.663 7.134	7.513
C	12.604 12.392 13.344	12.78	473 417 431	440	6.764 7.24 7.319	7.017

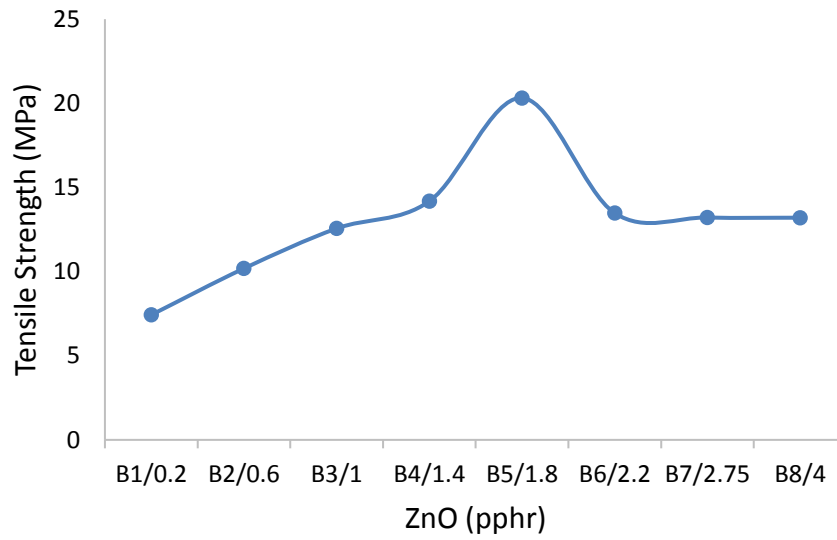


Figure 5.7: Tensile Strength of (B) Compounds.

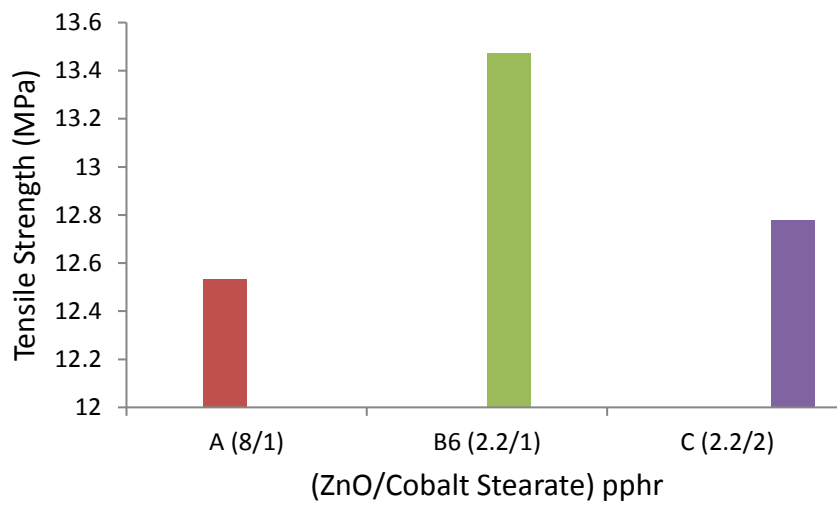


Figure 5.8: Tensile Strength of (A), (B6) and (C) Compounds.

5.2.4.2 Modulus at 300%

The results of (B) compounds are presented in Figure (5.9). The modulus at 300% increases progressively with increasing nano-ZnO level from 0.2 pphr up to a maximum value at 1.8 pphr due to increase the crosslink density. But the modulus at 300% decreases with increasing nano-ZnO beyond 1.8 pphr because of the relation between zinc oxide and crosslink density and the negative effect of increasing the crosslink density on the elasticity of the compound after 1.8 pphr of the concentration of nano-ZnO.

In order to study the effect of nano-ZnO on modulus at 300%, the results are compared with that of (A) compound. The maximum modulus of nano-ZnO is 11.102 MPa and it is greater than the modulus of (A) compound which is 9.858 MPa. But when the modulus for (A) compound is compared with (B6) compound (see Figure (5.10)), the modulus for (B6) compound is less than that for (A) compound because the crosslink density for (B6) compound is less than that for (A) compound. Also from Figure (5.10), the modulus for (C) compound is less than modulus for (B6) compound because it has crosslink density less than (B6) compound.

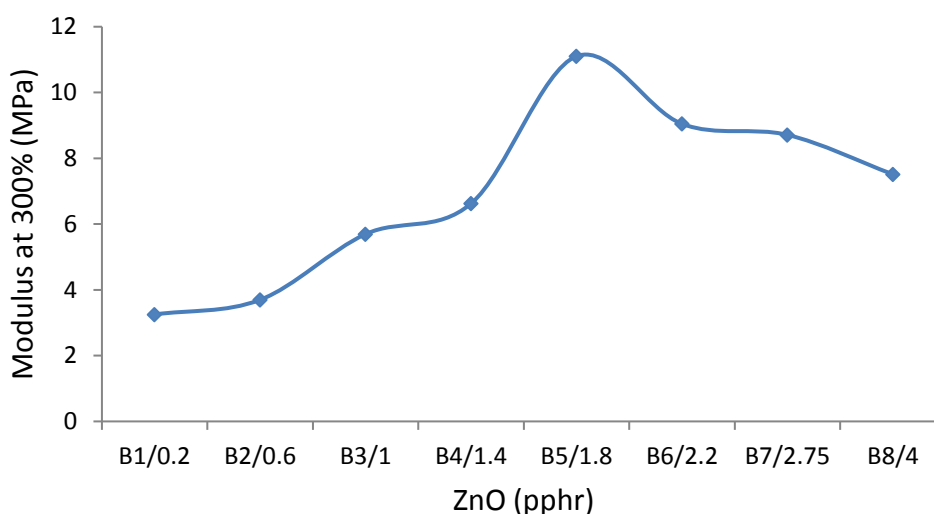


Figure 5.9: Modulus at 300% of (B) Compounds.

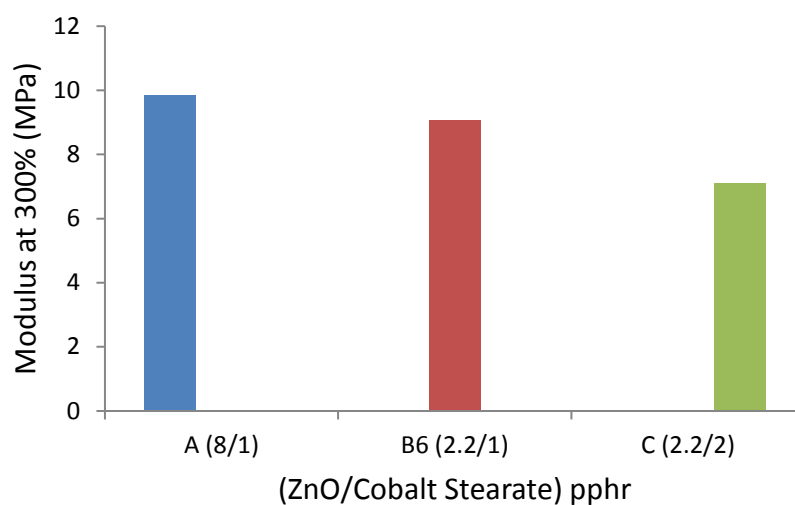


Figure 5.10: Modulus at 300% of (A), (B6) and (C) Compounds.

5.2.4.3 Elongation at Break

According to the results of (B) compounds in the Table (5.5) and Figure (5.11), the elongation at break decreases with increasing nano-ZnO level. This observation is attributed to the increase in crosslink density with increasing nano-ZnO level leading to a reduction in molecular chain mobility. Also, the comparison of the elongation at break for (A), (B6) and (C) compounds is shown in Figure (5.12). From this figure the elongation at break decreased with increasing the crosslink density.

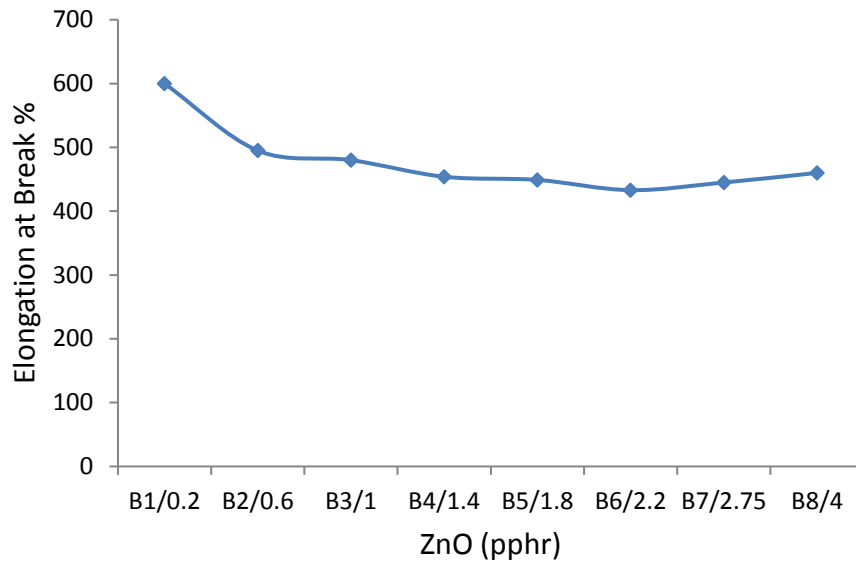


Figure 5.11: Elongation at Break of (B) Compounds.

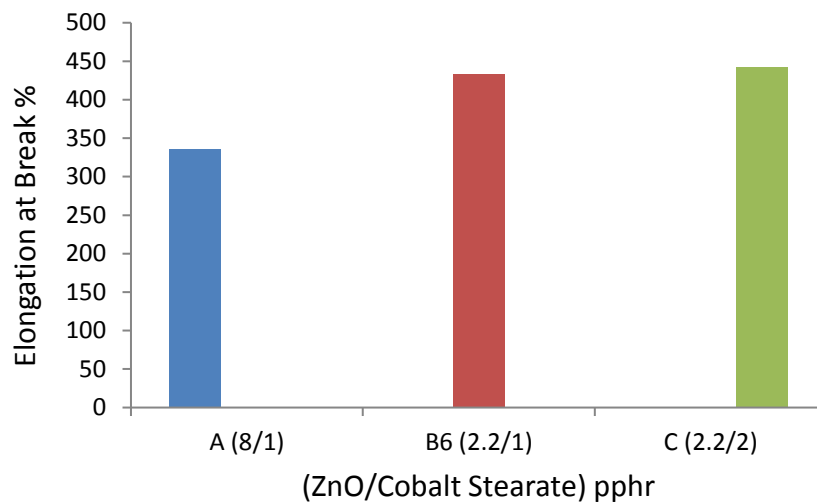


Figure 5.12: Elongation at Break of (A), (B6) and (C) Compounds.

In this work, the effect of the adhesion force between rubber and steel tire cord with increasing temperature was studied and improved in (A) compound, which is used as a standard in State Company for Tire Industry in Najaf without a decrease in other properties. Table (5.6) shows the values dependence in state company.

Table 5.6: The Laboratory Control Limit for 1k4100 (A) Compound.

No.	Property	Value
1.	Hardness (IRHD)	52 - 59
2.	Torque (Lb.In)	Min. 25
3.	Tensile Strength (MPa)	Min. 15
4.	Elongation	Min. 400
5.	Modulus at 300%	Min. 10

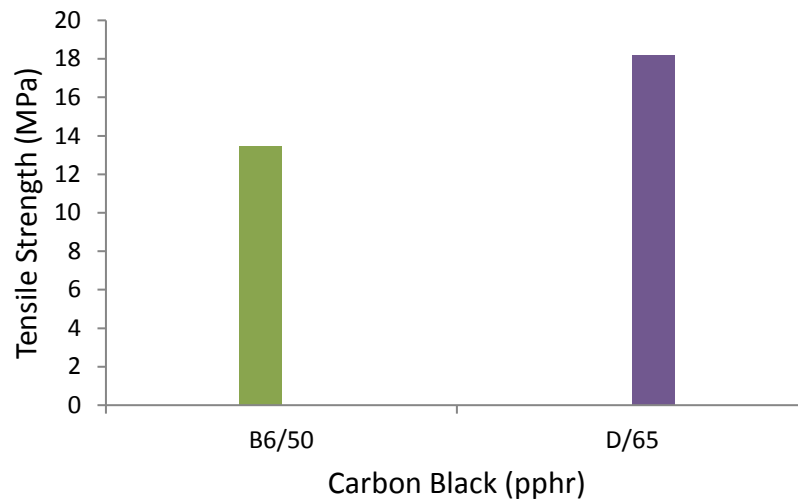
The (B6) compound has the best adhesion force but its tensile strength is 13.475 Mpa and its modulus at 300% is 9.046 Mpa which is less than the values dependence in state company according to Table (5.6).

To improve the tensile properties of (B6) compound, the level of carbon black in D compound must be increased from 50 pphr to 65 pphr in order to use it a filler to increase the strength up to 65 pphr [3], this is according to the work of Saad [26] who presented that increasing carbon black level leads to increase tensile properties.

The results of the tensile test for (D) compound are summarized in Table (5.7) and presented in Figure (5.13). Also, the results of modulus at 300% of (D) compound are shown in Figure (5.14). From these figures, the (D) compound has tensile strength and modulus are greater than (B6) compound because increasing carbon black level leads to increase the rubber-filler interactions and decrease the elongation at break. This behaviour is due to the restriction of the chains mobility resulting from the physical crosslinks introduced by the carbon black (see Figure (5.15)). Also, the hardness increases with increasing carbon black level for the same reason of increasing tensile properties (see Figure (5.16)).

Table 5.7: Results of Tensile Test of (D) Compound.

Compound	Tensile Strength (MPa)	Tensile Strength Average (MPa)	Elongation at Break %	Elongation at Break Average%	Modulus at 300% (MPa)	Modulus at 300% Average (MPa)
D	19.194 19.759 15.609	18.187	462 481 708	450	10.442 10.253 10.108	10.267

**Figure 5.13:** Comparing the Tensile Strength Between (B6) and (D) Compounds.

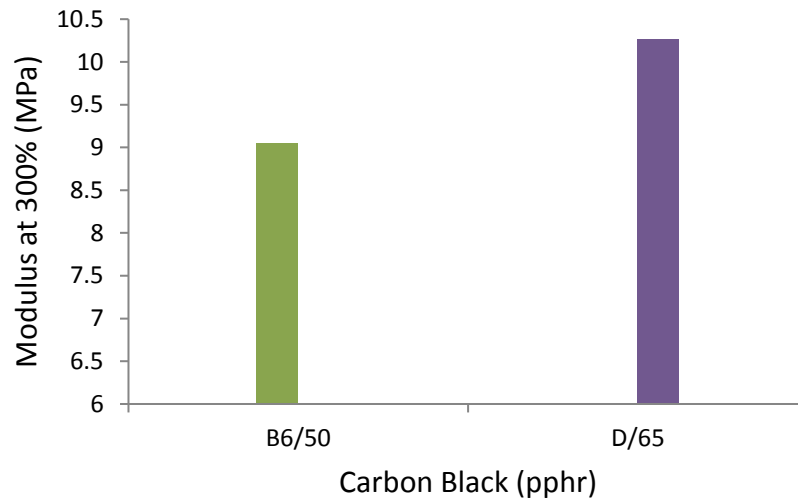


Figure 5.14: Comparing the Modulus at 300% Between (B6) and (D) Compounds.

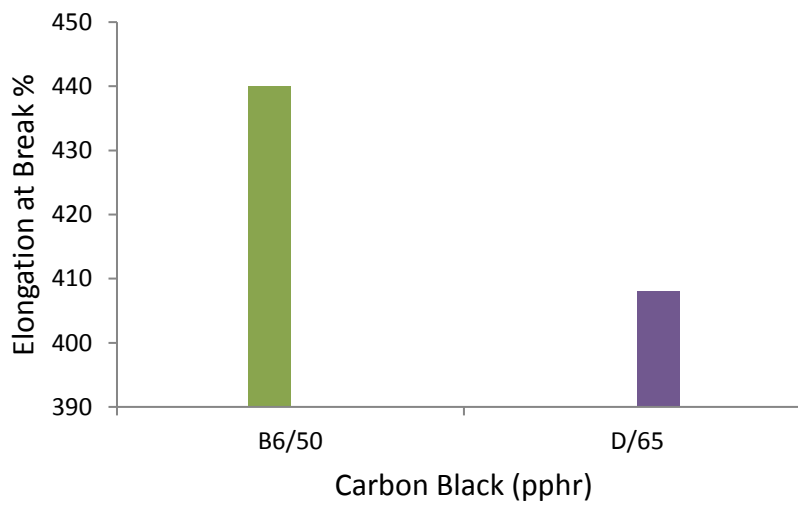


Figure 5.15: Comparing the Elongation at Break Between (B6) and (D) Compounds.

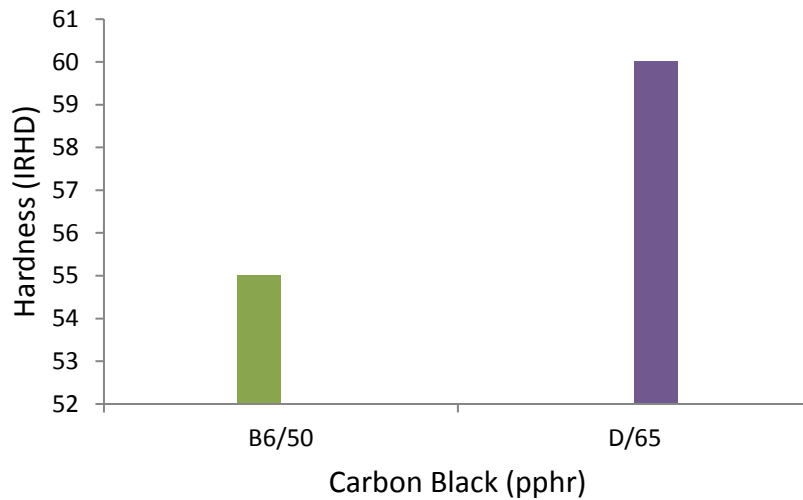


Figure 5.16: Comparing the Hardness Between (B6) and (D) Compounds.

Table (5.8) and Figure (5.17) show the effect of increasing carbon black concentration on the pull-out force. The pull-out force increases in (D) compound due to increasing crosslink density and other mechanical properties which lead to shrinkage rubber compound around steel cord and difficulty in extruding cord out.

Table 5.8: Pull-Out Force Values at Different Temperature of (D) Compound.

Compound Sample	D			
	25	50	75	100
Pull-out Force (N)	315.867	284.157	263.205	247.912

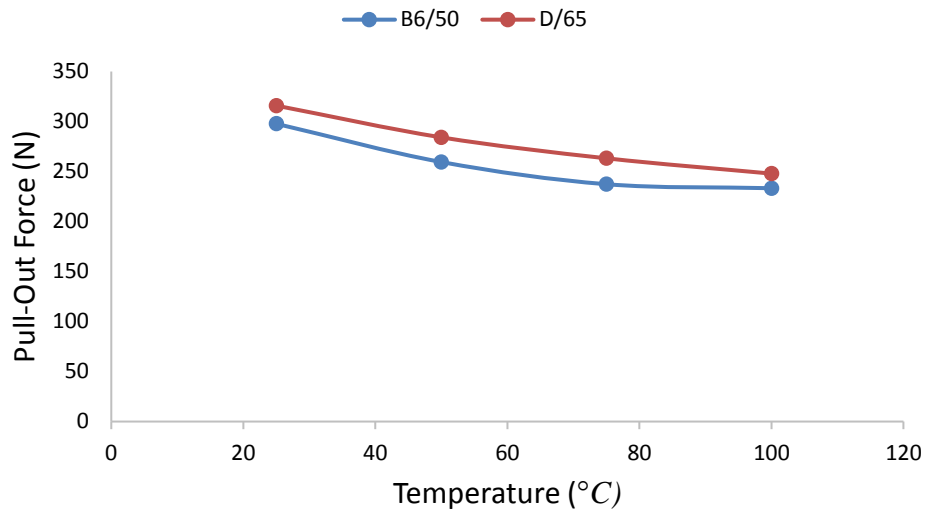


Figure 5.17: Comparing the Pull-Out Force Between (B6) Compound and (D) Compound.

5.3 Numerical Simulation Part

Numerical simulation FEM is a modern and sophisticated method that is used to reduce the effort and time in addition to reducing the experiment tests which is lead to reducing the total costs by reducing the materials needed for conducting these practice tests.

Therefore, the FEM was used in this study to estimate the pull-out-force which is needed to pull out the wire of steel from the mass of rubber for all types of compounds using ANSYS APDL. Vr 16.1 to make comparison between the numerical results and the experimental results.

A simplified model was made by taking a rubber block with a dimension of 25 mm×12.5 mm×12.5 mm that containing one cord of steel, which should be taken into account, as adhesion test works on pull one wire and records the value of the force. The same procedure then performs for all wires to take the average force value. Figure (5.18) shows the steps for moving wire along rubber block and finally to extrude out.

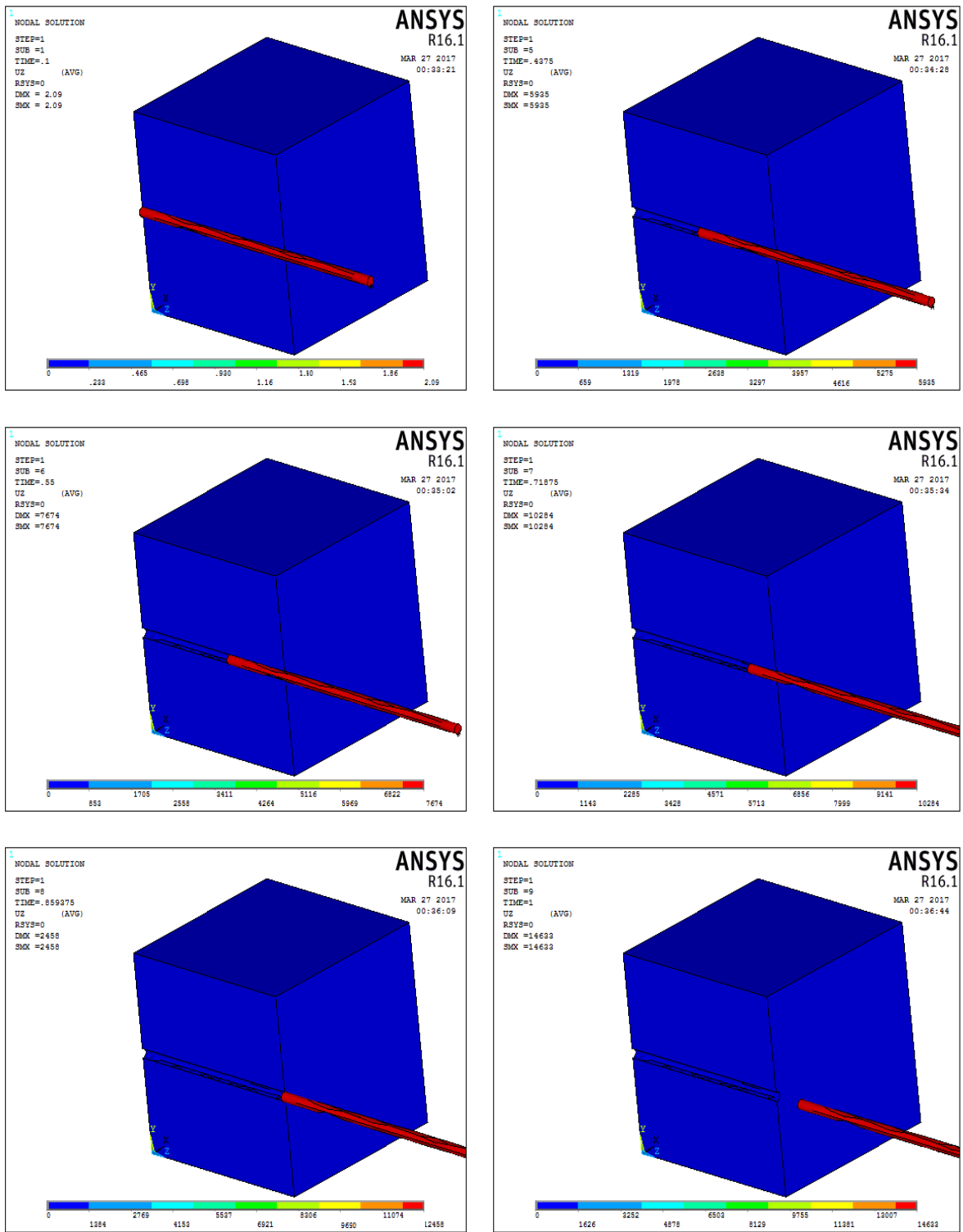


Figure 5.18: Moving Cord in Rubber Block.

In Table (5.9) the results of the numerical work and error percentage between the numerical and experimental works are listed. Figure (5.19) also shows the comparison between the numerical and experimental pull-out force results in steel cord of (B) compounds. The numerical results depend on the mechanical properties obtained from the tensile of rubber compounds. From these values, it can be concluded that any increase in tensile strength and elastic modulus leads to increase the pull-out force.

The maximum force can be seen in (B5) compound because this compound has a maximum tensile strength and elastic modulus as shown by experimental work. In experimental work, although its tensile strength and elastic modulus are greater than (B6) compound, the (B5) compound has a pull-out force less than the (B6) compound. This is because (B5) compound has a high crosslink between molecular rubber which increases the tensile strength and makes shrinkage in a rubber compound. This leads to making cracks in rubber compound and hence easily movement of cord in rubber compound is obtained.

Figure (5.20) shows the comparison between the numerical and experimental pull-out force results in steel cord for A, B6, C and D compounds. The percentage error is presented in Table (5.9).

Table 5.9: Pull-Out Force of Experimental and Numerical Works with Percentage Error Between Them.

Samples	Experimental Pull-out Force (N)	Numerical Pull-Out Force (N)	Error %
A	280.9	285	1.4
B1	142.85	150	4.7
B2	185.06	200	7.4
B3	231.59	240	3.5
B4	250.66	300	16.4
B5	265.26	330	19.6
B6	297.72	310	3.9
B7	215.75	280	22.9
B8	210.37	270	22
C	267.8	287	6.6
D	315.86	350	9.7

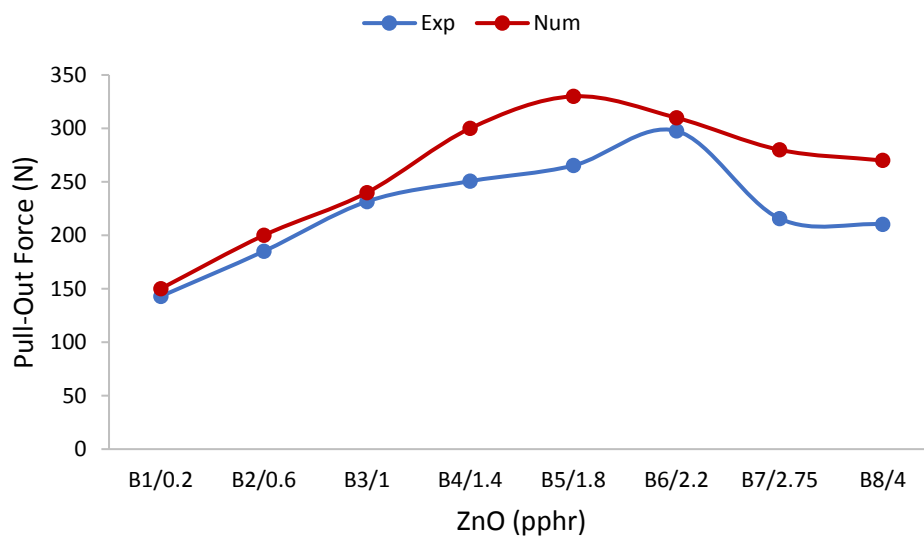


Figure 5.19: Comparison Between Numerical and Experimental Pull-Out Force of (B) Compounds.

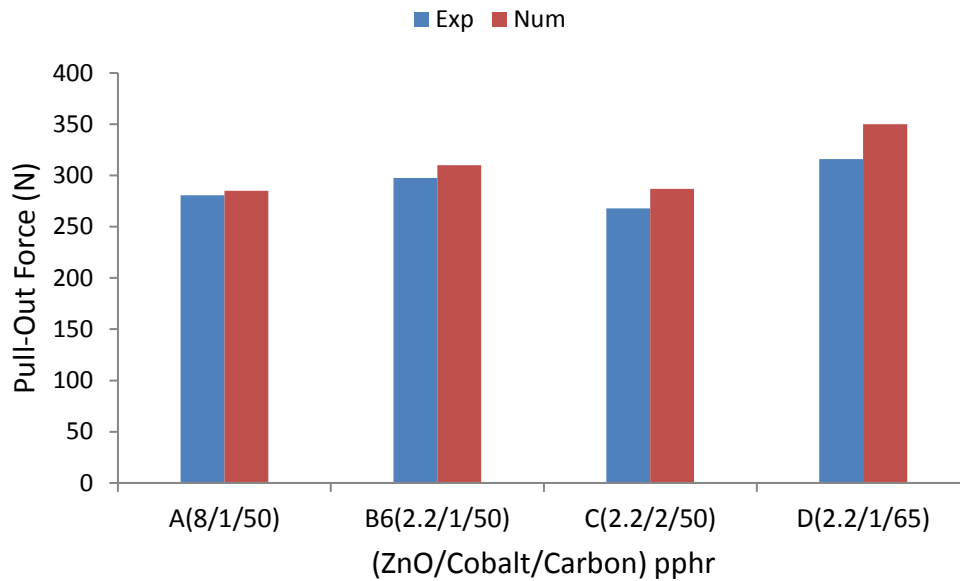


Figure 5.20: Comparison Between Numerical and Experimental Pull-Out Force of (A), (B6), (C) and (D) Compounds.

The maximum pull-out force in the experimental and numerical results is in the (D) compound. By comparing (D) compound with (A) compound, which is used in State Company for Tire Industry in Najaf, Figure (5.21) and Figure (5.22) show the appearance of the rubber compound with effect pull-out force in steel cord. From these figures, it can be seen the different between Von-Mises stress distribution on the rubber block. The stress in (A) compound is 0.144 Pa and in (D) compound is 0.0597 Pa but the pull-out force in (A) compound is less than that in (D) compound and this causes (A) compound to have a less stress comparing with (D) compound. These results mean that the stress depends on the specification of rubber compound. The elasticity of (D) compound is greater than that of (A) compound because the elongation at break is greater in (A) compound according to Tables (5.5) and (5.7). Also, the stresses are cumulative and they depend on the speed of moving cord, when the force is high the stresses do not have enough time to cumulative.

The space between rubber block and wire after extrusion gives an indication about adhesion between them. In Figure (5.21), it can be observed

that the space is greater than that in Figure (5.22). This means that the adhesion force in (A) compounds is less than that in (D) compound because the wire is easily moved.

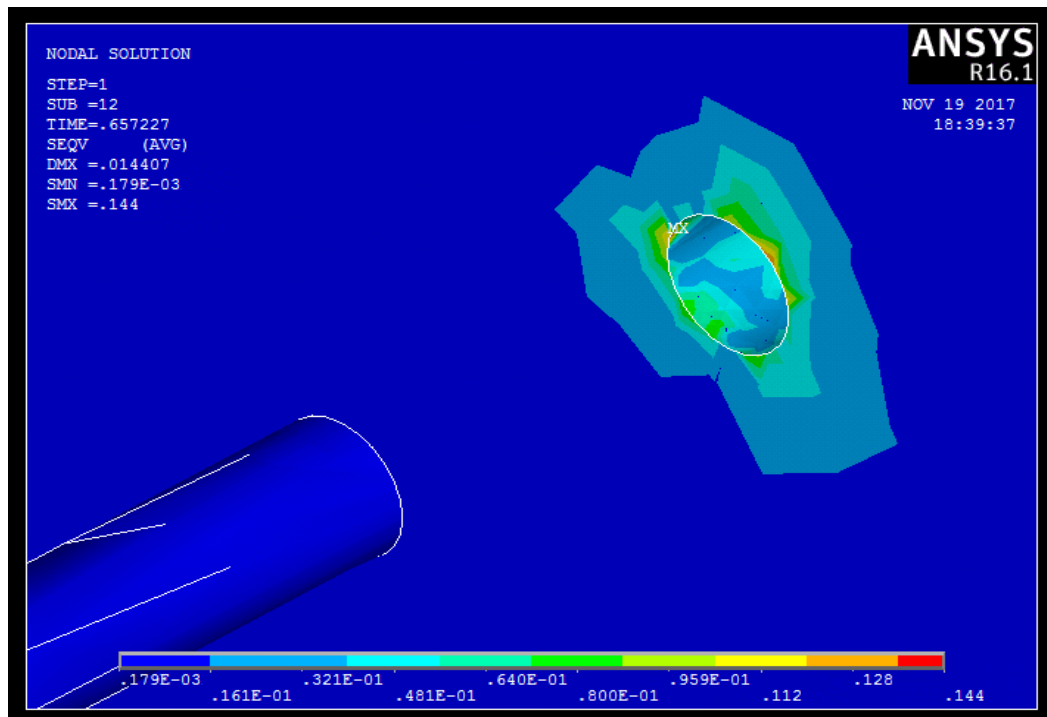
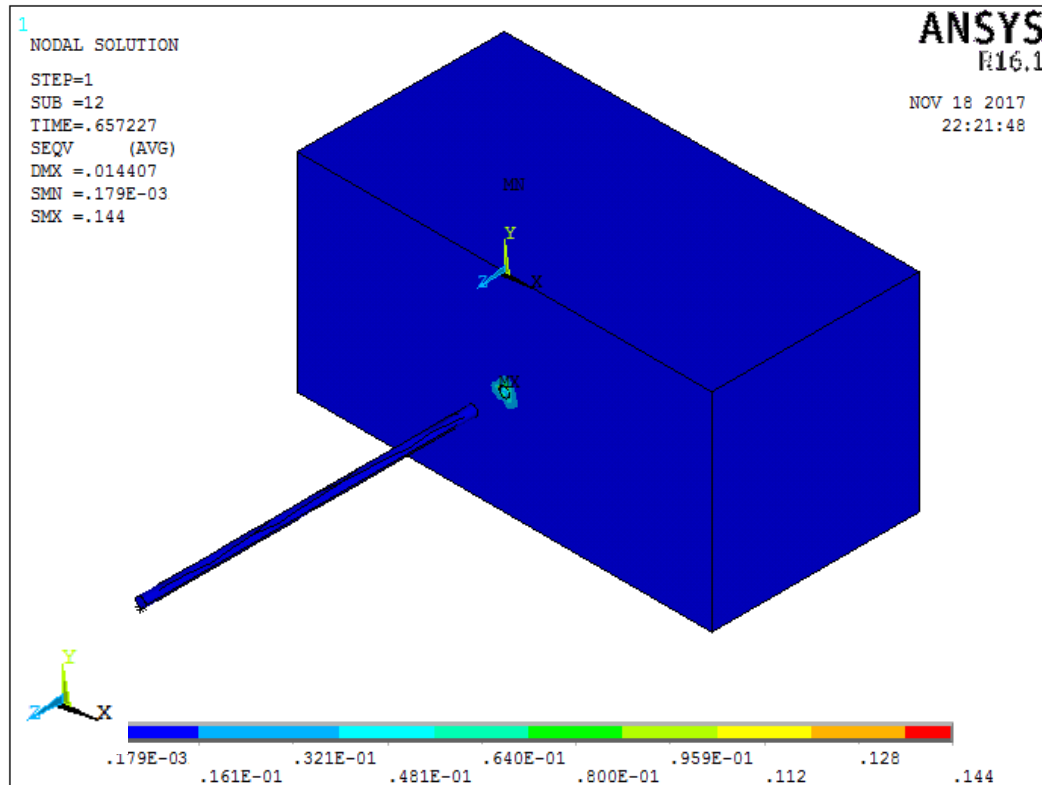


Figure 5.21: Steel Wire in (A) Rubber Block After Extrusion.

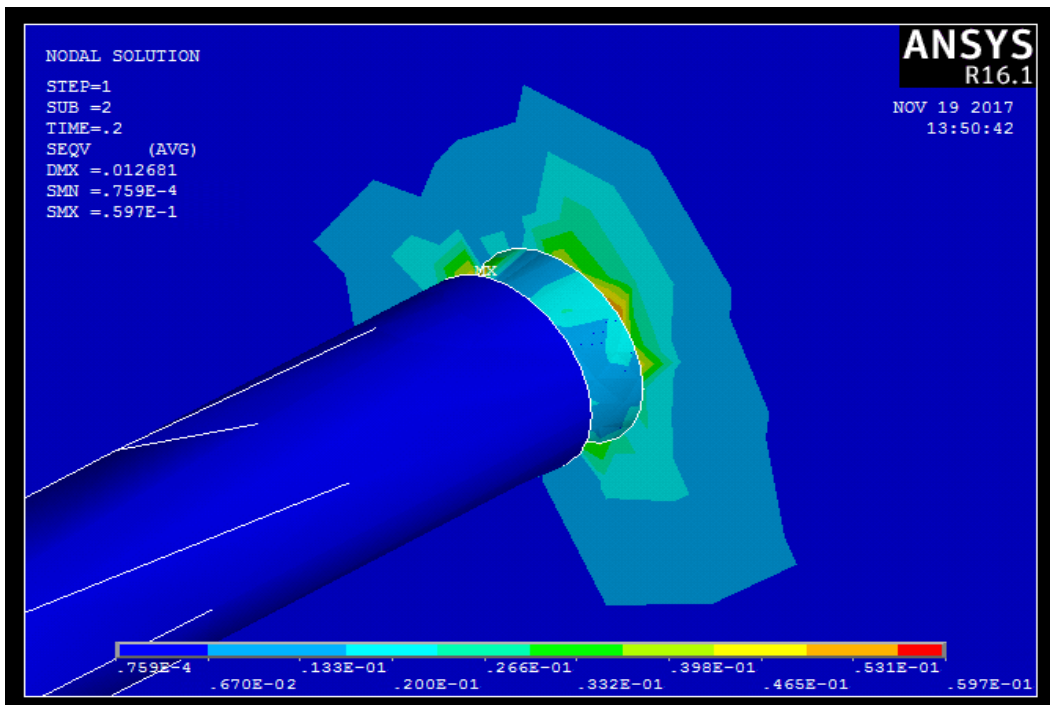
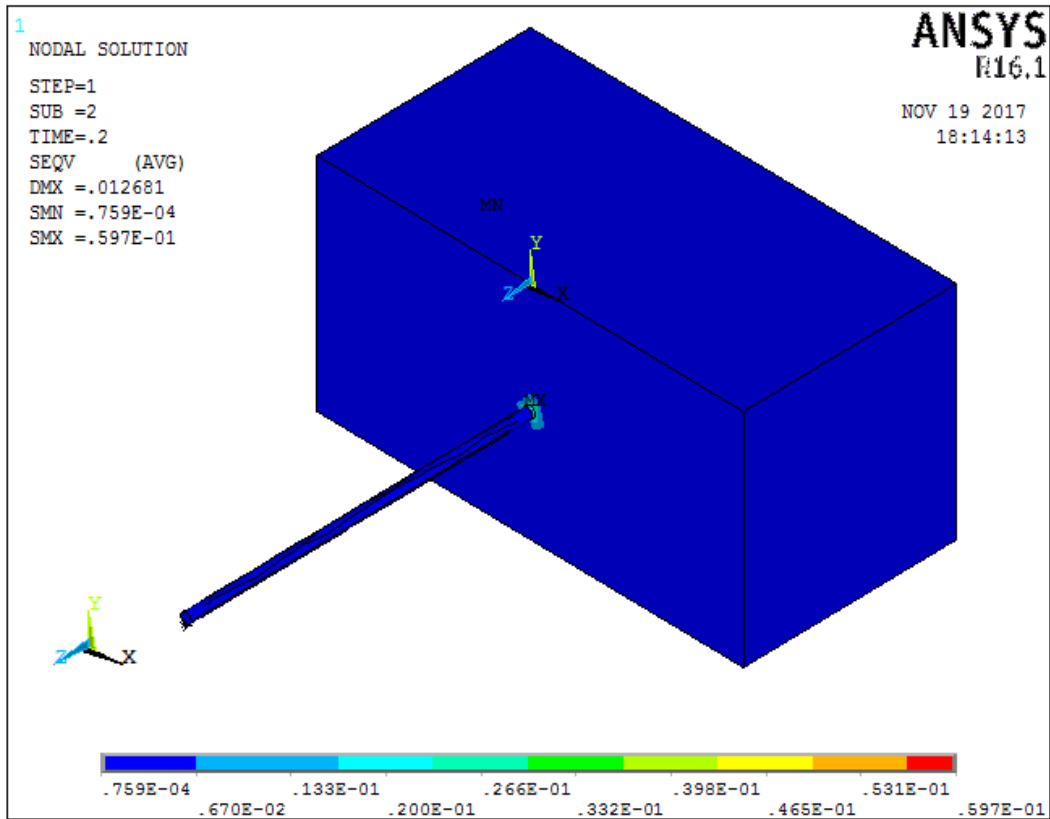


Figure 5.22: Steel Cord in (D) Rubber Block After Extrusion.



CHAPTER SIX
CONCLUSIONS AND
RECOMMENDATIONS

CONCLUSIONS AND RECOMMENDATIONS

6.1 Conclusions

Extensive experimental and numerical simulation of pull-out force for steel cord embedded in a rubber compound has been implemented in this work. The effect of replacing conventional ZnO by nano-ZnO and changing percentage of the materials in a recipe on the pull-out force are investigated numerically and experimentally. The effects of the temperature on adhesion force, cure characteristics, tensile properties and hardness are investigated experimentally.

The general conclusions of this work can be outlined as follows:

1. The replacing of the conventional ZnO by nano-ZnO into natural rubber composite gives a number of advantages:
 - Improving the adhesion force by 21 %.
 - Improving the tensile strength by 45.11 %.
 - Reducing the amount of zinc oxide by 72.5 %.
 - Reducing the cost of the compounds due to the price of nano-ZnO which is approximately equal to the price of conventional ZnO.
2. Improving the pull-out force in numerical work by 22.8%.
3. Von-Mises stress distribution along the rubber compound in the (D) compound is less than that in the (A) compound by 58.5 %.

6.2 Recommendations

Several recommendations can be suggested for future work, they can be outlined in the following points:

1. Using the SBR instead of SMR20.
2. Using the bead wire instead of the steel wire cord in (D) compound.
3. Test the dumbbell specimen at different temperatures to predict the pull-out force with temperature effect in numerically work.



REFERENCES

REFERENCES

- [1] Bergstrom J.S., Boyce M.C., “Deformation of Elastomeric Networks: Relation between Molecular Level Deformation and Classical Statistical Mechanics Models of Rubber Elasticity”, *Macromolecules*, Vol. 32, pp. 3795-3808, 2001.
- [2] Crowther B., “Handbook of Rubber Bonding”, Rapra Technology Limited, 2003.
- [3] Erman B., Mark J. E., Roland C. M., “The Science and Technology of Rubber”, 4th Edition, Elsevier, Tokyo, 2013.
- [4] Gent A. N., Walter J. D., “The Pneumatic Tire”, The University of Akron, 2006.
- [5] Harakuni P., “Mechanistic Investigation of the Sulfide Layer Formed at the Rubber-Steel Tire Cord Interface”, M.Sc. Thesis, Department of Chemical and Materials Engineering of the College of Engineering, University of Cincinnati, 2007.
- [6] GENT A. N., “Engineering with Rubber: How to Design Rubber Components”, Hanser Publishers, 2012.
- [7] Donald H. Buckley, “Surface Effects in Adhesion Friction, Wear and Lubrication”, Amsterdam, Oxford, New York, 1981.
- [8] Stuart J. R. Baum, “Chemistry a Life Science Approach”, Second Edition, Macmillan Publishing Co., New York, 1980.
- [9] William C. Wake, “Adhesion and Formation of Adhesives”, Applied Science Publishers Limited, London, 1976.

- [10] Rodgers B., “Rubber Compounding”, Chemistry and Applications, Marcel Dekker, New York, 2004.
- [11] Heideman G., Noordermeer J. W. M., Datta R.N., “Reduced Zinc oxide Levels in Sulphur Vulcanization of Rubber Compounds”, Enschede, 2004.
- [12] ASTM D1415, Standard Test Method for Rubber Property-International Hardness.
- [13] Payne A. R., Scott J. R. “Engineering Design with Rubber”, Maclaren and Sons London, 1960.
- [14] ASTM D412, Standard Test Methods for Vulcanized Rubber and Thermoplastic Elastomers-Tension.
- [15] Gyung S. J., Min H. H., Gon S., “Effect of ZnO Contents at the Surface of Brass-Plated Steel Cord on the Adhesion Property to Rubber Compound”, Korean J. Chem. Eng., Vol. 16, pp. 248-252, 1999.
- [16] Jeon G. S., Seo G., “Influence of Cure Conditions on the Adhesion of Rubber Compound to Brass-plated Steel Cord. Part II. Cure Time”, J. Adhesion, Vol. 76, pp. 223-244, 2001.
- [17] Al Maamori M. H., Hasan H. G., “Investigation of Parameters Affecting Adhesion Between Metal Wire and Nylon Fiber to Rubber”, M.Sc. Thesis, College of Engineering, University of Babylon, 2002.
- [18] Jeon G. S., Seo G., “Effects of Cure Levels on Adhesion Between Rubber and Brass in the Composites Made Up of Rubber Compound and Brass-Plated Steel Cord”, Korean J. Chem. Eng., Vol. 20, No. 3, pp. 496-502, 2003.
- [19] Jamshidi M., Afshar F., Mohammadi N., Pourmahdian S., “Study on Cord/Rubber Interface at Elevated Temperatures by H-pull Test Method”, Applied Surface Science, Vol. 249, pp. 208-215, 2005.

- [20] Jeon G. S., “Adhesion Between Rubber Compounds and Ternary-Alloy-Coated Steel Cords, Part I: Effect of Cobalt Plating Amount in Ternary-Alloy-Coated Steel Cords”, *J. Adhesion Sci. Technol.*, Vol. 19, No. 6, pp. 445-465, 2005.
- [21] Jeon G. S., Kang U. I., Jeong S. W., Choi S. J., Kim S. H., “Adhesion Between Rubber Compounds and Ternary-Alloy-Coated Steel Cords. Part II: Effects of Sulfur and Cobalt Salt in Rubber Compounds”, *J. Adhesion Sci. Technol.*, Vol. 19, No. 15, pp. 1325-1348, 2005.
- [22] Wang J., Chen Y., “Application of Nano-Zinc Oxide Master Batch in Polybutadiene Styrene Rubber System”, *Journal of Applied Polymer Science*, Vol. 101, pp. 922-930, 2006.
- [23] Sahoo S., Kar S., Ganguly A., George J. J., Bhowmick A. K., Maiti M., “Effect of Zinc Oxide Nanoparticles as Cure Activator on the Properties of Natural Rubber and Nitrile Rubber”, *Journal of Applied Polymer Science* Vol.105, pp.2407-2415, 2007.
- [24] Jeon G. S., “Adhesion Between Rubber Compounds Containing Various Adhesion Promoters and Brass-Plated Steel Cords. Part I. Effect of Sulfur Loading in Rubber Compounds”, *Journal of Adhesion Science and Technology*, Vol. 22, pp.1223-1253, 2008.
- [25] Taghvaei-Ganjali S., Malekzadeh M., Abbasian A., Khosravi M., “Effects of Different Activator Systems on Cure Characteristics and Physicomechanical Properties of a NR/SBR Blend”, *Iranian Polymer Journal*, NO. 18-5, pp. 415-425, 2009.
- [26] Saad I. S., Fayed M. Sh., Abdel-Bary E. M., “Effects of Carbon Black Content on Cure Characteristics, Mechanical Properties and Swelling

Behaviour of 80/20 NBR/CIIR Blend”, Aerospace Sciences & Aviation Technology (ASAT), Vol. 13, pp. 06, 2009.

[27] Mottaghi M., Khorasani S. N., Esfahany M. N., Farzadfar A., Talakesh M.M., “Comparison of the Effect of Nano-ZnO and Conventional Grade ZnO on the Cross-Linking Densities of NR/BR and NR/SBR Blends”, Journal of Elastomers and Plastics, vol. 44, NO. 5, pp.443-451, 2012.

[28] Buytaerta G., Luob Y., “Study of Cu–Zn–Co Ternary Alloy-Coated Steel Cord in Cobalt-Free Skim Compound”, Journal of Adhesion Science and Technology, Vol. 28, No. 16, pp.1545-1555, 2014.

[29] Morton M., “Rubber Technology”, Springer Netherlands, 1999.

[30] ASTM D3182, Standard Practice for Rubber-Materials, Equipment, and Procedures for Mixing Standard Compounds and Preparing Standard Vulcanized Sheets.

[31] Engineering Documentation of tire industry, Manual 7-Volume 1D, Libretary Equipment, Dunlop International Projects Limited, 1989.

[32] ASTM D1349, Standard Practice for Rubber-Standard Temperatures for Testing.

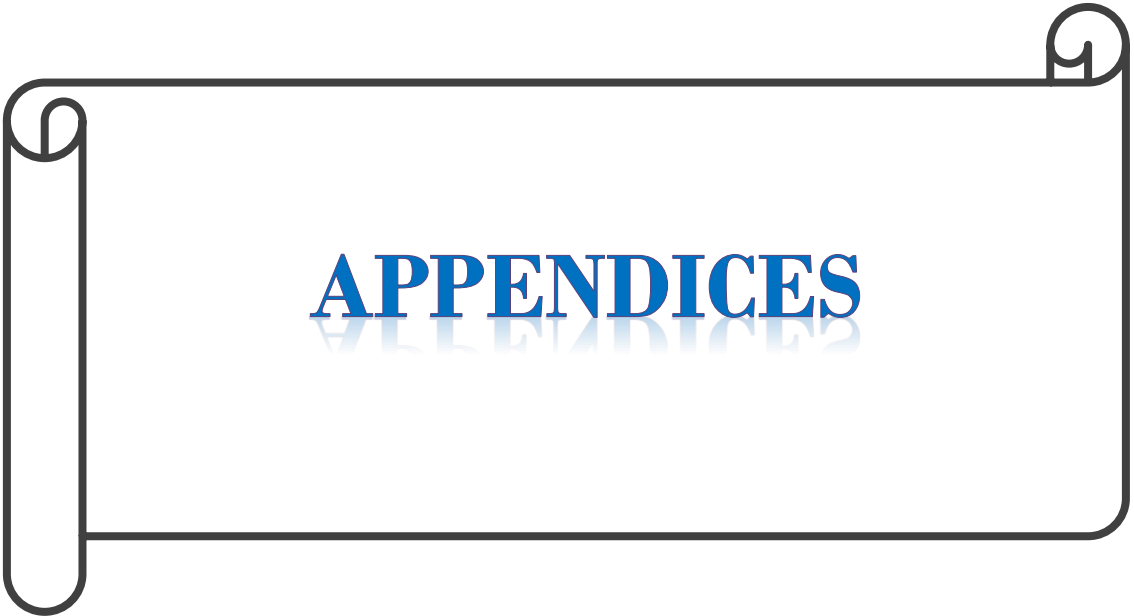
[33] ASTM D2229, Standard Test Method for Adhesion Between Steel Tire Cords and Rubber.

[34] Nakasone Y. and Yoshimoto S., “Engineering Analysis with ANSYS Software”, Department of Mechanical Engineering, Tokyo University of Science, 2006.

[35] K. Roy, Md. N. Alam, S. K. Mandal, S. C. Debnath, “Surface Modification of Sol–Gel Derived Nano Zinc Oxide (ZnO) and the Study of its Effect on the

Properties of Styrene–Butadiene Rubber (SBR) Nanocomposites”, J Nanostruct Chem, Vol.4, pp.133-142, 2014.

[36] G. Seo, G. Soo, “Adhesion Between Rubber Compound and Copper-Film-Plated Steel Cord and Rubber Compound Containing Adhesion Promotor”, J. of the Korean Institute of Chemical Engineering, Vol. 37, No. 6, pp. 834-868, 1999.



The Results of Tensile Test

Strain	Stress (MPa)
0	0.028
1	0.194
1	0.277
2	0.416
3	0.472
4	0.583
5	0.694
6	0.721
7	0.805
8	0.86
9	1.027
10	1.082
11	1.138
12	1.165
13	1.248
14	1.304
15	1.359
16	1.387
17	1.443
18	1.47
19	1.526
20	1.581
21	1.609
22	1.692
23	1.72
24	1.748
25	1.803
26	1.831
27	1.887
28	1.914
29	1.942
30	1.998
31	2.025
32	2.053
33	2.081
34	2.136
35	2.164
36	2.22
37	2.247
38	2.275
39	2.358
40	2.358
41	2.386
42	2.441

Strain	Stress (MPa)
44	2.539
45	2.584
46	2.63
47	2.676
48	2.721
49	2.767
50	2.813
51	2.859
52	2.904
53	2.95
54	2.996
55	3.042
56	3.089
57	3.135
58	3.181
59	3.227
60	3.274
61	3.32
62	3.367
63	3.413
64	3.46
65	3.506
66	3.553
67	3.6
68	3.647
69	3.694
70	3.741
71	3.788
72	3.835
73	3.882
74	3.929
75	3.976
76	4.024
77	4.071
78	4.119
79	4.166
80	4.214
81	4.261
82	4.309
83	4.357
84	4.405
85	4.452
86	4.5
87	4.548

89	4.645
90	4.693
91	4.741
92	4.789
93	4.838
94	4.886
95	4.934
96	4.983
97	5.032
98	5.08
99	5.129
100	5.178
101	5.227
102	5.275
103	5.324
104	5.373
105	5.422
106	5.472
107	5.521
108	5.57
109	5.619
110	5.669
111	5.718
112	5.768
113	5.817
114	5.867
115	5.916
116	5.966
117	6.016
118	6.066
119	6.116
120	6.166
121	6.216
122	6.266
123	6.316
124	6.366
125	6.416
126	6.467
127	6.517
128	6.568
129	6.618
130	6.669
131	6.719
132	6.77
133	6.821
134	6.872

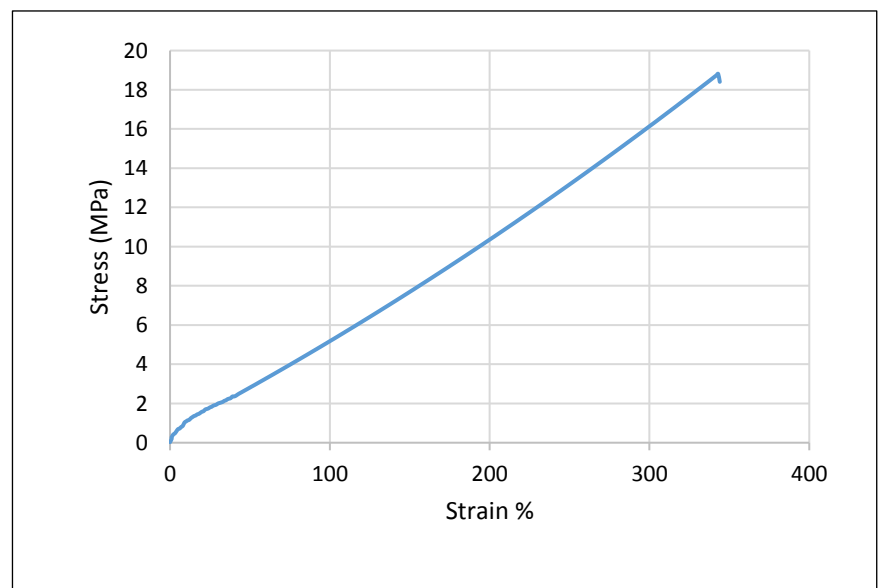
136	6.973
137	7.024
138	7.075
139	7.127
140	7.178
141	7.229
142	7.28
143	7.332
144	7.383
145	7.434
146	7.486
147	7.538
148	7.589
149	7.641
150	7.693
151	7.745
152	7.796
153	7.848
154	7.9
155	7.952
156	8.005
157	8.057
158	8.109
159	8.161
160	8.214
161	8.266
162	8.319
163	8.371
164	8.424
165	8.476
166	8.529
167	8.582
168	8.635
169	8.688
170	8.741
171	8.794
172	8.847
173	8.9
174	8.953
175	9.006
176	9.06
177	9.113
178	9.167
179	9.22
180	9.274
181	9.327

182	9.381
183	9.435
184	9.489
185	9.542
186	9.596
187	9.65
188	9.704
189	9.759
190	9.813
191	9.867
192	9.921
193	9.976
194	10.03
195	10.084
196	10.139
197	10.194
198	10.248
199	10.303
200	10.358
201	10.413
202	10.467
203	10.522
204	10.577
205	10.632
206	10.688
207	10.743
208	10.798
209	10.853
210	10.909
211	10.964
212	11.02
213	11.075
214	11.131
215	11.186
216	11.242
217	11.298
218	11.354
219	11.41
220	11.466
221	11.522
222	11.578
223	11.634
224	11.69
225	11.746
226	11.803
227	11.859

228	11.916
229	11.972
230	12.029
231	12.085
232	12.142
233	12.199
234	12.256
235	12.312
236	12.369
237	12.426
238	12.483
239	12.541
240	12.598
241	12.655
242	12.712
243	12.77
244	12.827
245	12.884
246	12.942
247	13
248	13.057
249	13.115
250	13.173
251	13.231
252	13.288
253	13.346
254	13.404
255	13.462
256	13.521
257	13.579
258	13.637
259	13.695
260	13.754
261	13.812
262	13.871
263	13.929
264	13.988
265	14.046
266	14.105
267	14.164
268	14.223
269	14.282
270	14.341
271	14.4
272	14.459
273	14.518

274	14.577
275	14.636
276	14.696
277	14.755
278	14.815
279	14.874
280	14.934
281	14.993
282	15.053
283	15.113
284	15.173
285	15.232
286	15.292
287	15.352
288	15.412
289	15.473
290	15.533
291	15.593
292	15.653
293	15.714
294	15.774
295	15.834
296	15.895
297	15.956
298	16.016
299	16.016
300	16.077
301	16.138
302	16.199
303	16.259
304	16.32
305	16.381
306	16.442
307	16.504
308	16.565
309	16.626
310	16.687
311	16.749
312	16.81
313	16.872
314	16.933
315	16.995
316	17.056
317	17.118
318	17.18
319	17.242

320	17.034
321	17.336
322	17.49
323	17.552
324	17.614
325	17.676
326	17.739
327	17.801
328	17.864
329	17.926
330	17.989
331	18.051
332	18.114
333	18.177
334	18.24
335	18.302
336	18.365
337	18.428
338	18.491
339	18.555
340	18.618
341	18.681
342	18.744
343	18.808
344	18.406



الخلاصة

ان التصاق المطاط المترالكب إلى سلك الفولاذ يعتبر ذات أهمية قصوى في الصناعات المطاطية. لذلك فان الدراسة الحالية تهدف إلى دراسة تأثير أكسيد الزنك النانوي والتأثير الحراري على قوة الالتصاق بين المطاط والاسلاك في الاطارات. وتشمل هذه الدراسة محورين مهمين: دراسة عمليه وعددية.

نتيجة لارتفاع درجة الحرارة اثناء عمل ودوران الإطارات، فإن الطاقة الناتجة من الالتصاق ستختلف إذا ما قورنت مع حالتها الأولية. ومن اجل دراسة الالتصاق بين المطاط والسلك في درجات الحرارة المرتفعة، تم استخدام طريقة اختبار السحب T. في هذا البحث عينات الالتصاق T تحسب عند درجات حراره بقيم مختلفة وهي 25، 50، 75، 100 درجة مئوية. كما تم في هذا البحث دراسة خصائص الشد والصلادة لمساعدة المصمم في تصميم اطارات أفضل وأقوى.

تم تحضير احدى عشر عجنة مختلفة من المترالكبات المطاطية باستخدام مدلفنة مزدوجة ومكابس مختبرية لدراسة تأثير المكونات الشائعة على الالتصاق بين المطاط والاسلاك في الاطارات. احدى هذه العجنات تحتوي على أكسيد الزنك الاعتيادي كمنشط بتركيز 8 pphr (جزء من مائة من وزن المطاط). ثمان عجنات تحتوي على أكسيد الزنك النانوي بتركيز (0.2, 0.6, 1, 1.4, 1.8, 2.2, 2.75, 4 pphr). بينما العجتان المتبقيتان تحتويان على أكسيد الزنك النانوي بتركيز 2.2 pphr، احدهما تحتوي على 2pphr ستيارات الكوبلت بدلا من 1pphr والأخرى تحتوي على 65 pphr من اسود الكربون بدلا من 50 pphr.

الدراسة العددية تم اجراءها باستخدام طريقة العناصر المحددة والتي تم تنفيذها من خلال البرنامج الحسابي المعروف باسم ANSYS الاصدار 16.1 وذلك لحساب قوة السحب المطلوبة لسحب سلك الفولاذ من كتلة المطاط ولجميع أنواع المترالكبات. نتائج الدراسة العددية تمت مقارنتها مع النتائج العملية. وقد أظهرت النتائج التي تم الحصول عليها من الدراسة العملية أن زيادة درجة الحرارة تؤدي إلى تقليل الالتصاق بين المطاط والسلك في الإطارات. كذلك اظهرت النتائج ان استبدال أكسيد الزنك الاعتيادي بأكسيد الزنك النانوي يؤدي إلى تحسين قوة الالتصاق بنسبة 21٪، وتقليل كمية أكسيد الزنك بنسبة 72.5٪ وقوة الشد بنسبة 45.11٪. كما أنه يؤدي إلى خفض تكلفة المترالكبات لأن سعر أكسيد الزنك النانوي يساوي تقريبا سعر أكسيد الزنك الاعتيادي.

بالإضافة الى ما تقدم ذكره فقد اظهرت النتائج العددية أن قوة السحب تزداد بنسبة 22.8%. عند مقارنتها مع النتائج العملية، حيث وجد أن نسبة الخطأ هي 9.7%.



جمهورية العراق
وزارة التعليم العالي والبحث العلمي
جامعة كربلاء - كلية الهندسة
قسم الهندسة الميكانيكية

دراسة تأثير أكسيد الزنك النانوي والتعتيق الحراري على قوة الالتصاق بين المطاط المتراكب وأسلاك الفولاذ

رسالة مقدمة الى كلية الهندسة - جامعة كربلاء كجزء من متطلبات نيل درجة الماجستير في علوم
الهندسة الميكانيكية - ميكانيك تطبيقي

من قبل

سجى قاسم محمد

بكالوريوس ٢٠١٣

بإشراف

الاستاذ المساعد الدكتور عبد الكريم عبد الرزاق الحمداني

الاستاذ المساعد الدكتور مهند لفنة الوائلي